**Marine resurge sequences at Flynn Creek impact structure, Tennessee, USA.**

by

Leticia Pacetta De Marchi

A thesis submitted to the Graduate Faculty of
Auburn University
in partial fulfillment of the
requirements for the Degree of
Master of Science

Auburn, Alabama
August 4, 2018



Approved by

Dr. David T. King Jr., Chair, Professor of Geology
Dr. Willis Hames, Professor of Geology
Dr. Jens Ormö, Research Scientist

## Abstract

The Flynn Creek crater is a 3.8-km impact structure located in the Eastern Highland Rim geological province of Jackson County, Tennessee (36°17’ N; 85°40’ W), which displays a central uplift, breccia-filled crater moat, and terraced crater rim. The impact occurred during Late Devonian in an epicontinental shelf setting wherein the target Upper Ordovician bedrock carbonates were just beginning to be overlain by thin, basal beds of the transgressive Upper Devonian Chattanooga Shale. Granulometric (line-logging) and statistical studies of two drill cores, FC77-3 and FC67-3, shows that the crater-filling deposits containing four distinct parts. The lower part is interpreted as fall back sediments, which are followed by slump deposits from the crater rim. The middle part is a mixing zone between slump from the collapsing central peak and initial marine resurge flow. This is capped by a normally graded breccia unit formed by marine resurge water. Petrographic study of thin sections including microprobe analyses reveals that the crater moat-filling breccia contain two types of melt: a previously known grey silica melt, that shows a cryptocrystalline texture and commonly containing euhedral dolomitic inclusions, and a previously unknown phosphatic amber-colored melt, that occurs in association with elements from the base of the Chattanooga Shale supporting the idea that the shale was already being deposited at the time of the impact. Uneven distribution of petrographic components throughout the drill cores on opposite sides of the central uplift may suggest possible ejecta asymmetry.

## Acknowledgments

This work was supported by The Barringer Fund for Meteorite Impact Research and by National Aeronautics and Space Administration, through the Planetary Geology and Geophysics program (NASA PPG NNH14AY73I). The author also thanks research and travel support provided by Auburn University College of Sciences and Mathematics (COSAM), Auburn University Geosciences Advisory Board (GAB), and Alabama Geological Society (AGS). Also, thank for the essential support from the USGS Astrogeology Science Center, Flagstaff, especially Tenielle Gaither, who was really helpful on providing us a space to work during line-logging process, cutting and mailing of samples, and essential information about drill-cores. I am also very thankful for the essential help from Steven Jaret, on interpreting data and field trip, Dr. Hames, on acquiring and interpreting microprobe data, and Dr. Jens Ormö, also my co-advisor, on collecting and interpreting data since the beginning and until the end of the current project. Thanks to all colleagues, staff, faculty members, friends, and family for their encouragement and motivation. My last, and more important, thanks are for my advisor Dr. King, who I had the pleasure to work with during these past two years. Thanks for the opportunity to study at Auburn, for your patience and your support. I am really grateful for all things that I have learned from you, not just about science but also about life. You and Lucille were the base for my performance and made me feel home since my first day in a different country.

Table of Contents

List of Tables

List of Figures

# Introduction

The current study aims to describe and interpret infilling deposits at Flynn Creek crater, which is an impact structure formed in Upper Ordovician flat-lying carbonate rocks, approximately 382 million years ago (during Devonian), in a shallow marine environment. All data were collected from two drill cores, FC77-3 and FC67-3, which are located in the crater moat on opposite sides of the central uplift, enabling comparison of infilling processes in different regions of the crater. Results are here compared to other marine impact craters and also provide additional information to complement other drill core studies within the central uplift carried out by Adrian et al. (2018). This thesis is part of a collaborative project between Auburn University and USGS Astrogeology Science Center in Flagstaff, which is focused on study of the USGS Flynn Creek drill core collection.

Following the *Meteoritics and Planetary Science's* format, this thesis comprises two papers separated in two different chapters. The first one, "Evidence of marine resurge sequences at Flynn creek impact structure, Tennessee," is currently in review and describes the sedimentary sequences and their interpreted depositional processes, by using granulometric and statistical analyses. The second paper, "Petrographic characteristics of crater moat-filling breccia, Flynn creek impact structure, Tennessee." focus on a microscopic and chemical characterization of impact related features and deposit by studying thin sections that are allocated along both drill cores. Tables with complete thin section volumetric data have been added as an appendix, because these data are not displayed in the main text.

## CHAPTER 1

# Evidence of marine resurge sequences at Flynn Creek impact structure, Tennessee.

L. De Marchi[1], J. Ormö[2], D. T. King Jr.[1*], D. R. Adrian[1], J. J. Hagerty[3], and T. A. Gaither[3]

[1]Deptartment of Geosciences, Auburn University, Auburn, Alabama 36849

[2]Centro de Astrobiología (INTA-CSIC), Madrid, Spain

[3]USGS, Astrogeology Science Center, Flagstaff, Arizona 86001

*Corresponding author. Email: kingdat@auburn.edu

**Abstract -** In the history of impact crater studies, Flynn Creek was the first impact crater to have been shown to have formed in a marine target setting. In addition to water, the Flynn Creek target sequence included mainly poorly consolidated limestones and dolomites, thus promoting a complex morphology for this relatively small (3.8-km wide) crater. Granulometric (line-logging) analysis of two drill cores, FC77-3 and FC67-3, situated respectively in the northwestern and southeastern quadrants of the Flynn Creek impact structure's crater-moat area, reveals that the ~ 27-m thick crater moat-filling breccia consists of three distinct parts. These three parts are distinguished primarily on the bases of sorting, grain size, and number of clasts per meter, and secondarily on the bases of clast lithology and shape. The lower part is interpreted to represent initial fall-back deposition, which was followed rapidly by slump deposits mainly from the crater rim. The middle part is interpreted as a zone of mixing between slump from the collapsing

central peak and in-coming marine resurge. And, the upper part is a normally graded and relatively well-sorted deposit, which is capped by a thin, graded (calcarenite to calcisiltite) bed and is interpreted as the main marine resurge deposit. Resurge at Flynn Creek has a rapid transition into secular sediments (i.e., overlying, dark marine shales). Graded resurge deposits at the two study locations within the crater moat are approximately 10-m thick and both indicate the process of suspension flow containing a considerable amount of entrained water. We think this finding shows the target water depth to have been at least as deep as o 10 m, which was suggested by previous research. In an impact in shallower water, this target sedimentary sequence would have produced a resurge with strong debris-flow characteristics, which is not the case at Flynn Creek. Our interpretations are supported by comparisons with resurge deposits at other marine-target impact structures, namely Lockne, Tvären, Wetumpka, and Chesapeake Bay, all of which formed at different relative target water depths.

## INTRODUCTION

Flynn Creek is a Late Devonian, ~3.8-km diameter, complex, marine-target impact structure, which occurs in the Eastern Highland Rim geological province of Jackson County, Tennessee (36°17’ N; 85°40’ W). Figure 1 shows the location of this impact structure within Tennessee, a simple geological map with crater-rim outline, and the two core-hole locations of the present study. Both these core holes are situated on opposite sides of the central uplift, in the moat just outside the central uplift area. Flynn Creek is one of the ‘original six’ impact craters identified on Earth (French and Short, 1968) and was the first impact crater to be identified as being of marine origin (Roddy, 1968). This impact structure formed approximately 382 million years ago in an epicontinental shelf setting wherein the target Upper Ordovician bedrock

carbonates were just beginning to be overlain by thin, basal beds of the transgressive Upper Devonian Chattanooga Shale. The numerical age determination of 382 million years comes from

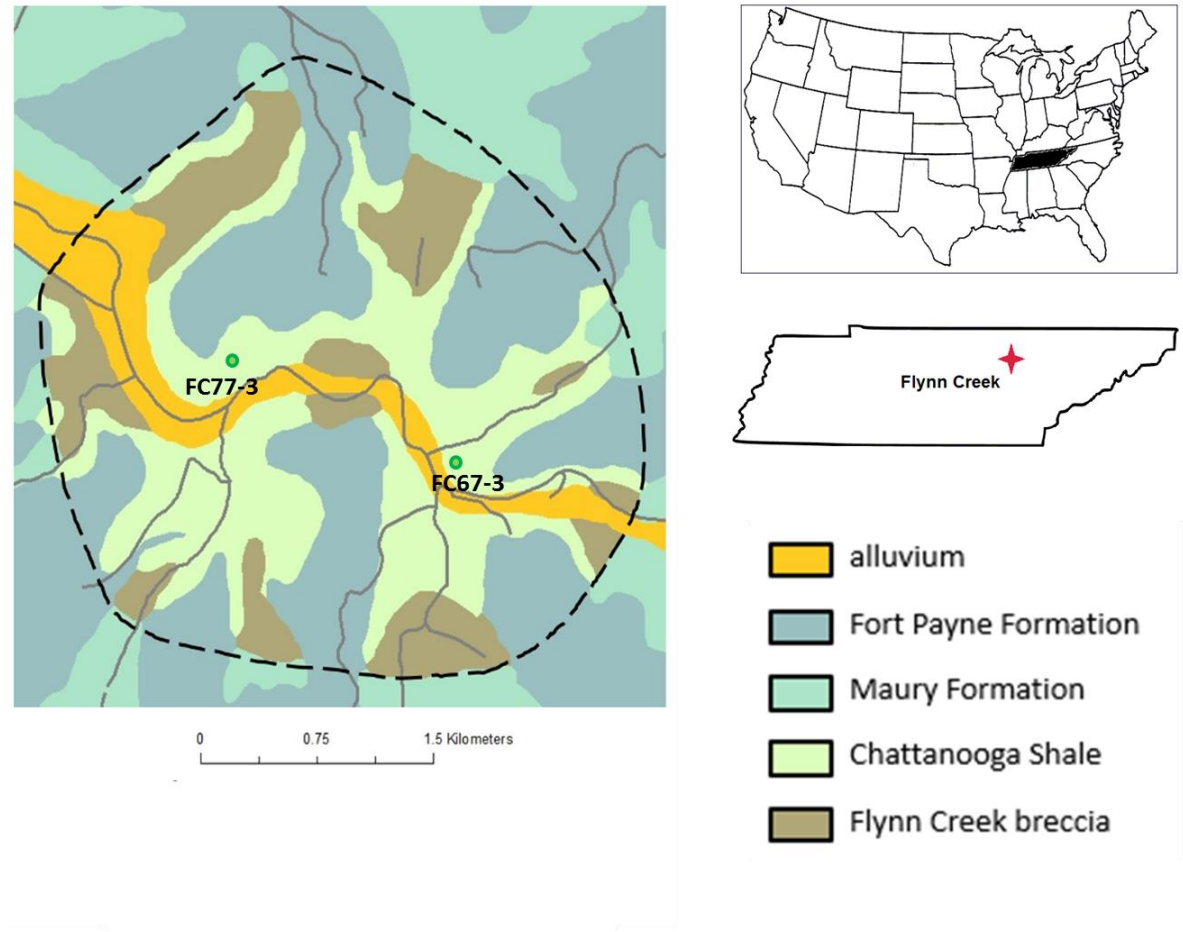


Figure 1. Geological map of Flynn Creek impact structure and vicinity. Inset maps show the location of the state of Tennessee in the contiguous United States and the location of the Flynn Creek impact structure. Green dots show the locations of two core holes of this study, FC-67-3 and FC77-3. Colors (see legend in figure) show the main stratigraphic units, including alluvium and the Fort Payne Formation (post-impact chert), Maury Formation (post-impact shale), Chattanooga Shale (post-impact shale) and Flynn Creek breccia (crater-filling unit). The outcrops of the Catheys-Leipers Formation in the rim area and the Stones River and Knox Groups in the central uplift area are too small to show at this scale. The central uplift is indicated by the central outcrop of Flynn Creek impact breccia (brown), which caps the exposure of the central peak and its flanks. Dashed line shows the asymmetric limit of the impact structure's rim according to Roddy (1968), who conducted extensive field studies in the area. Modified from the Flynn Creek map on the U.S. Geological Survey Mineral Resources On-Line Spatial Database (mrdata.usgs.gov).

biostratigraphic age determinations of fresh conodont that originated in the sediment of the basal bed(s) of the Chattanooga Shale target and then were found and extracted from the matrix of the Flynn Creek breccia by Schieber and Over (2005). The initial study of Flynn Creek that provided proof of a marine impact origin was conducted by David R. Roddy as his doctoral research (Roddy, 1966). Roddy observed several lines of evidence that led him to an impact hypothesis for Flynn Creek, including intensive structural deformation restricted to the crater area and closely surrounding areas, concentric faults zones in the innermost rim and in interpreted crater walls, the size-graded breccia deposits partially filling the structure, and shatter cones in the central uplift area. After his doctoral program, Roddy continued field work at Flynn Creek (Roddy, 1968; 1979). In addition, a multi-year core-drilling campaign was conducted by the USGS in connection with Roddy's work at Flynn Creek (Roddy, 1980; Hagerty et al., 2013; Gaither et al., 2015). This protracted drilling program eventually produced 21 individual drill cores. Six cores were drilled during 1967, three during 1977, and 12 during 1978-1979 (Gaither et al., 2015). The entire drill-core collection is housed at the USGS Astrogeology Center in Flagstaff, Arizona.

The geological setting for Flynn Creek is relatively simple: the local Paleozoic strata have essentially no dip angle and there are very few local pre-impact structural features such as faults or folds in the area (Conant and Swanson, 1961). Figure 2 summarizes the target stratigraphy of the area, and shows the schematic stratigraphic position of the Flynn Creek breccia, an informal unit that occupies the crater moat. Figure 2 also schematically shows the characteristics of target lithologies, including limestone, dolostone, shale, and minor quartzose sands.

According to Roddy (1968; 1979), as a general rule, Flynn Creek's rim exposures are comprised of younger target strata (Cannon Limestone and the Catheys-Leipers Formation of the Upper Ordovician Nashville Group), whereas the central uplift is formed by older target strata (Middle Ordovician Stones River Group and Lower Ordovician Knox Group; Roddy, 1968; 1979; Evenick and Hatcher, 2007).

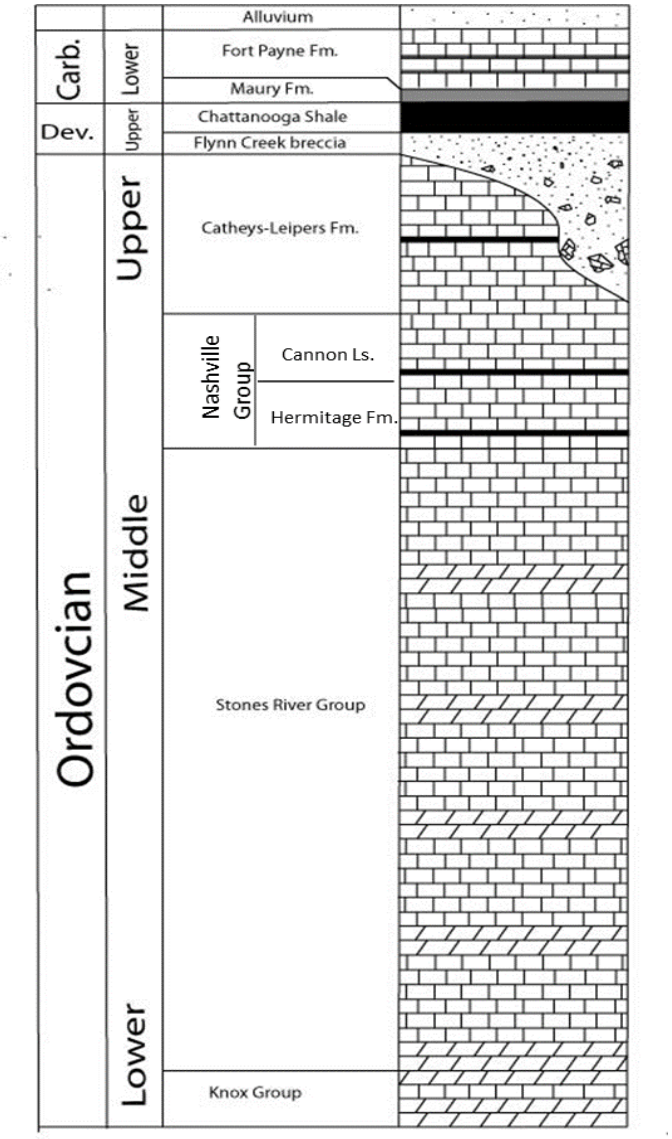


Figure 2. Stratigraphy of the target area of the Eastern Highland Rim geologic province (modified from Roddy, 1968).

Recently, a detailed examination of a core-hole on the western flank of the central uplift showed that the central uplift is draped by a thick layer of impact-related breccias of multiple origins (Adrian et al., 2017).

The informal Flynn Creek breccia, including both the central uplift breccia and the crater-filling moat breccia, is overlain by the Upper Devonian Chattanooga Shale, as are the undeformed target strata outside the impact structure area. Younger units, including the Lower Carboniferous Fort Payne Chert, overlie the Chattanooga Shale across the area.

The main objective of the present study is to explore the formation processes of the crater moat-filling breccia deposits at Flynn Creek. The two selected Flynn Creek drill cores are from locations on opposite sides of the central uplift area. Drill core FC77-3 is situated in the northwestern quadrant of the crater moat area, whereas drill core FC67-3 is situated in the southeastern quadrant of the crater moat area (Fig. 1). The present research uses standard techniques for analysis of the sedimentology of Flynn Creek's marine resurge breccia (i.e., line-logging and graphic analysis of line-logging data). These techniques have been used successfully for interpretation of early modification events within other marine target craters of comparable paleo-water depth (e.g., Lockne, Tvären, and the Chesapeake Bay Impact Structure (CBIS); Ormö et al., 2007; 2009).

## METHODOLOGY

The breccia deposits in drill cores FC77-3 and FC67-3 were analyzed for their clast lithologic type, shape, and long-axis grain size using the line-logging and allied, statistical data-treatment methods developed by Ormö et al. (2007; 2009). Ormö et al. applied this method to the study of resurge deposits within Lockne, Tvären, and Chesapeake Bay marine-target craters, in

accordance to the definition of resurge deposits as given by Ormö et al. (2007). The technique of Ormö et al. is a nondestructive, fast, and economic method.

The data are collected along a thin line drawn down the center of each piece of drill core (see example, Fig. 3). Each clast, greater than or equal to the cut-off size of 5 mm, which is touching the center line is assessed as to grain size (i.e., apparent long-axis length) and lithologic identity. Clasts less than 5-mm in long axis length were excluded mainly due the difficulty of accurate size measurement and in lithological determination (using hand lens and, if appropriate, acid droplets to distinguish calcite from dolomite in clasts). For each clast greater than the cut-off size, the depth within the drill core to the nearest 0.01 m was recorded also, in addition to the aforementioned grain size, shape, and lithology. Data were recorded continuously with depth, starting at the bottom of the moat-filling sequence in the instance of each drill core. Those data were stored in spreadsheet format for ease of use in the simple, deterministic statistics discussed below.

In this study, both for convenience and to be consistent with comparable data analysis of Lockne, Tvären, and Chesapeake Bay impact structures (Ormö, 2007, 2009), we used positive phi values, where phi = ($\log_2$ d), and d is the clast diameter in millimeters. For a statistical analysis of the 619 clast measurements from core FC77-3 and the 713 clast measurements from core FC67-3 the mean positive phi (φ) per meter, as well as the standard deviation for this mean value were calculated. The latter gives an indication for the size sorting. The number of clasts per meter was also plotted against depth within the drill cores.


Figure 3. Flynn Creek drill core FC77-3, core box number 4, depth 10.7-13.7 m, which has been marked with dashed lines to simulate the location of a pencil line for the line-logging method. The length of each slot within the box is two English feet, or 61 cm.

In our verbal descriptions of the sorting, terms like 'moderately well sorted' follows the sorting-terminology scheme of Folk (1974). Where the standard deviation of phi ($\sigma_\phi$) decreases, the degree of sorting among the clasts measured (i.e., above the cut-off size) increases.

Clast lithology was determined by hand-lens and, if in doubt, by checking the reaction with a droplet of HCl (where calcite limestone has a more obvious effervescence than dolostone) during the line-logging process. Clasts of limestone were distinguishable from dolostone (using a hand lens and checking reaction with a droplet of HCl where necessary). Shape of grains was visually estimated and classified using the four-stage roundness chart of rounded, sub-rounded, sub-angular, and angular given by Mazullo at al. (1988), and following a grain-shape comparator chart.

## RESULTS

Drill core FC77-3 from the northwestern quadrant of the crater moat area contains a moat-filling impact breccia sequence spanning a total thickness of 27.1 m, whereas FC-67-3 from the southeastern quadrant of the crater moat area displays a similar breccia sequence spanning a total thickness of 28.1 m, which includes an interval of missing drill-core from 33.9 to 37.6 m in depth. The logged clasts in the studied breccia sequences are – with few exceptions – either dolostone or limestone. But, we also counted other, different clasts types of only minor occurrence, including siltstone, calcarenite, melt particles, and fossil fragments.

Singular occurrences of rare clasts with "breccia in breccia" texture were observed in both drill cores. One such clast, (30 mm across) is located at 22.5 meters depth in FC77-3; and another is situated at 26.8 meters depth in FC63-3 (285 mm in size). Those were described as

matrix-supported intraformational clasts, with mm- and cm-size angular clasts in a light gray matrix, being similar to fall-back deposits, such as the inner Ries suevite of Osinski et al. (2016).

In drill core FC77-3, a total of 766 clasts were identified and counted. Of those, 683 (90%) were dolostone, 48 (6%) were limestone. In addition, 18 (2%) were fossil fragments, 11 (1%) were calcarenite clasts, and 6 (< 1%) were siltstone. In drill core FC67-3, a total of 623 clasts were identified and counted. Of those, 583 (94%) were dolostone, 36 (6%) were limestone, and 4 (< 1%) were fossil fragments. In addition to the aforementioned clast types, the fine grained fraction (<5mm) also contains shale clasts, chert fragments, melt particles, opaque grains, and fossil fragments.

The carbonate clasts could not be identified as to stratigraphic provenance owing to the many similar-appearing carbonate textures throughout the target stratigraphic section. In Figures 5 and 6, the occurrence of limestone and dolostone are plotted against depth for each drill core. As these plots clearly indicate, dolostone clasts dominate throughout both cores. However, in drill core FC67-3, small numbers of limestone clasts occur on all levels, whereas in drill core FC77-3 they are mainly confined to a section in the upper part of the core. In FC77-3, the very large clast is composed of limestone, whereas in FC67-3 it is composed of dolostone.

Whole-number values between 1 and 4 were given to describe the shape of each clast, where 1 is angular, 2 is sub-angular, 3 is sub-rounded, and 4 rounded, following the roundness chart given by Mazullo et al. (1988). In data from both drill cores, most of the values oscillate between sub-angular and sub-rounded with no main trend towards the top of the deposit (Fig. 4). FC77-3 shows a narrow interval between maximum and minimum mean roundness values, while FC67-3 displays a wider interval with most of the values slightly lower than FC77-3.

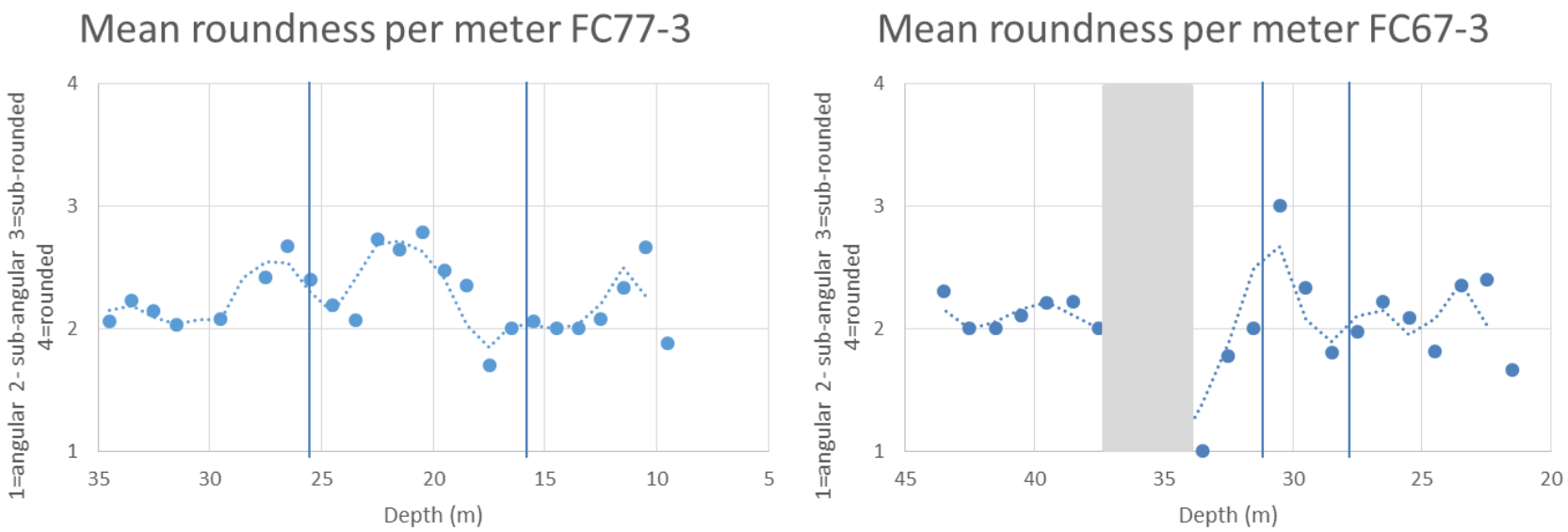


Figure 4. Plot of mean roundness per meter versus total depth in drill core FC77-3 (left) and FC67-3 (right).

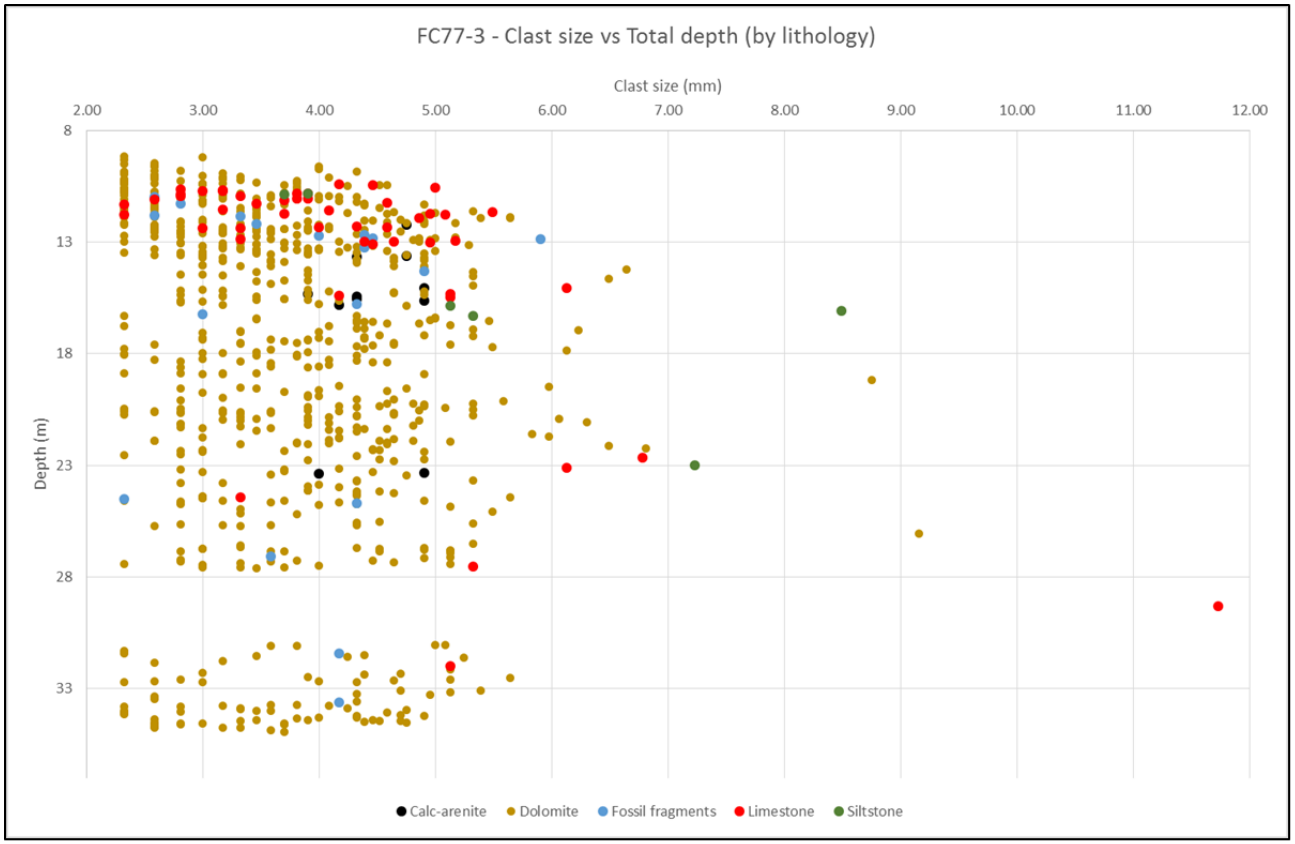


| FC77-3 | Calc-arenite | Dolomite | Limestone | Fossil fragment | Siltstone | total |
|---|---|---|---|---|---|---|
| Quantity | 11 | 683 | 48 | 18 | 6 | 766 |
| % | 1% | 90% | 6% | 2% | 1% | 100% |

Figure 5. FC77-3 drill core, plot of clast size versus total depth, by lithology. Dolomite and limestone clasts are coded by color. Upper, middle, and lower parts of the crater-filling unit are discussed in the text.

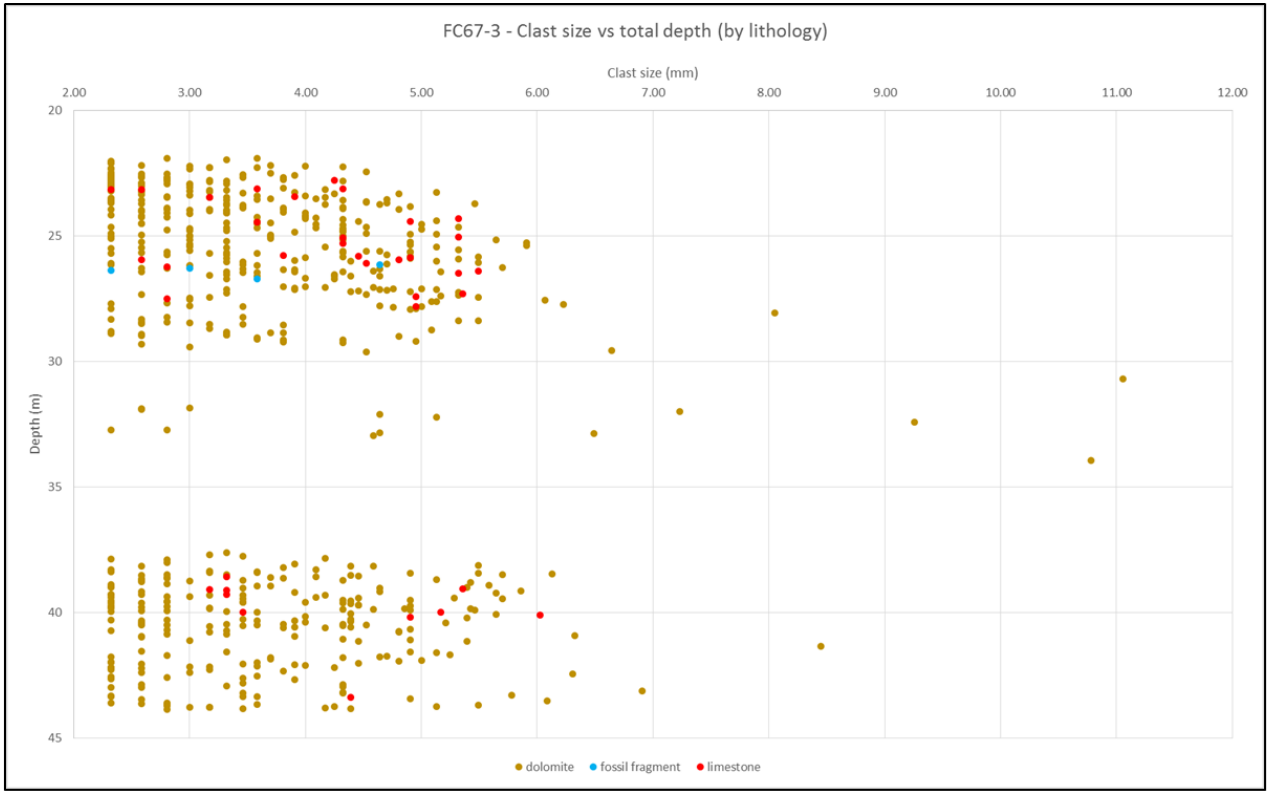


| FC67-3 | Dolomite | Limestone | fossil fragment | total |
|---|---|---|---|---|
| Quantity | 583 | 36 | 4 | 623 |
| % | 94% | 6% | 1% | 100% |

Figure 6. FC67-3 drill core, plot of clast size versus total depth, by lithology. Dolomite and limestone clasts are coded by color. Upper, middle, and lower parts of the crater-filling unit are discussed in the text.

Based on the clast-size variation and size-sorting results, the whole of the crater-filling sequence in both drill cores can be divided into three parts; the lower part is a relatively coarse and poorly sorted basal breccia. This is in turn overlain by an intermediate or middle breccia with varying sizes and sorting. This is overlaid by a better sorted, normally graded breccia unit. It is in this unit that the majority of limestone clasts appear. This normally graded unit passes upward into the more fine-grained sediments of an uppermost capping unit composed of graded calcarenites and calcisiltites. Because this capping unit consists of grains entirely under the cut-off limit of 5 mm (or $\phi \sim 2.3$), it is not shown on our graphs.

**Drill core FC77-3**

Figure 7 shows the vertical distribution of grain size, sorting, and clasts per meter for this drill core, which spans the depth range from 7.4 m (the Chattanooga Shale/Flynn Creek breccia contact) to 34.5 m (the Flynn Creek basal breccia/sub-crater contact). The vertical plots in Figure 7 show the overall trends can be separated into three main parts. In the lower part, from 34.5 to 28.5 m, the grain size increases significantly and the sorting overall is moderate to poor ($\sigma_\phi \sim 0.8$ to ~ 1.1). In the upper two meters of this lower part (30.5-28.5 m), the grain size is relatively large ($\phi \sim 11$). The number of clasts per meter declines sharply upward, especially within this coarse, 2-m zone. Grain support in this coarse zone is related to this sharp decline (matrix support dominates below the large clasts).

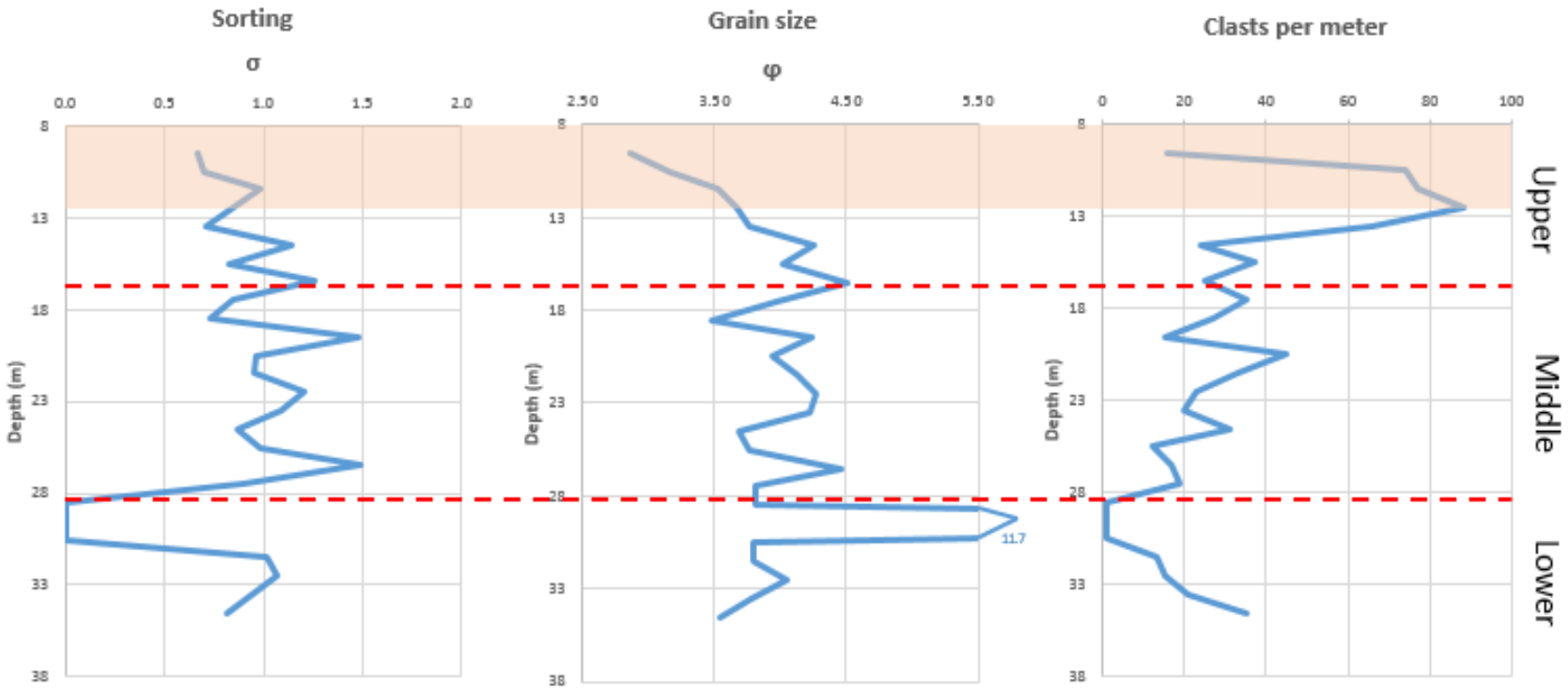


Figure 7. FC77-3 drill core, plots of key statistics versus depth in drill core. Upper, middle, and lower parts of the crater-filling unit are discussed in the text. Red shaded area indicates the portion where values are strongly affected by the 5-mm grain-size cut-off.

This lower coarse part is followed upwards by a middle part, spanning 28.5 to 17.5 m, where sorting fluctuates from moderately well sorted ($\sigma_\phi$ ~ 0.75) to poorly sorted ($\sigma_\phi$ ~ 1.5), in parity with grain-size shifts that range from $\phi$ ~ 3.5 to ~ 4.5, but without any major overall change (cf. with the underlying part). The number of clasts per meter increases upward within this middle part, which, in the absence of a clear decrease in grain size, is generally following an upward decline in matrix content.

The transition from the middle part to the upper part in drill core FC67-3 is mainly seen in the grain-size curve where there at 17.5 m is a shift in the trend towards a more obvious fining-up section. In this upper part, from 17.5 to 9.5 m, sorting continues to improve from $\sigma_\phi$ ~ 1.2 to ~ 0.7 (poorly sorted to moderately well sorted) and grain size falls off from $\phi$ ~ 4.5 to ~ 2.8. The number of clasts per meter increases drastically upwards in this part, but above 12.5 m depth cannot be considered reliable due to low numbers of counts as a consequence of the 5-mm cut-off size. In the interval from 9.5 m to the top of the drill core, there is a finer grained (i.e., calcarenite and calcisiltite) capping unit (7.4 m), where grain sizes are entirely below the cut-off size, but during line logging, we noted that these grains were well sorted and continuously size-graded (fining upward to the contact with the overlying Chattanooga Shale).

**Drill core FC67-3**

Figure 8 shows the vertical distribution of grain size, sorting, and clasts per meter for this drill core, which spans the depth range from 15.8 m (the Chattanooga Shale/Flynn Creek breccia contact) to 43.9 m (the Flynn Creek basal breccia/sub-crater contact). The logged section of this

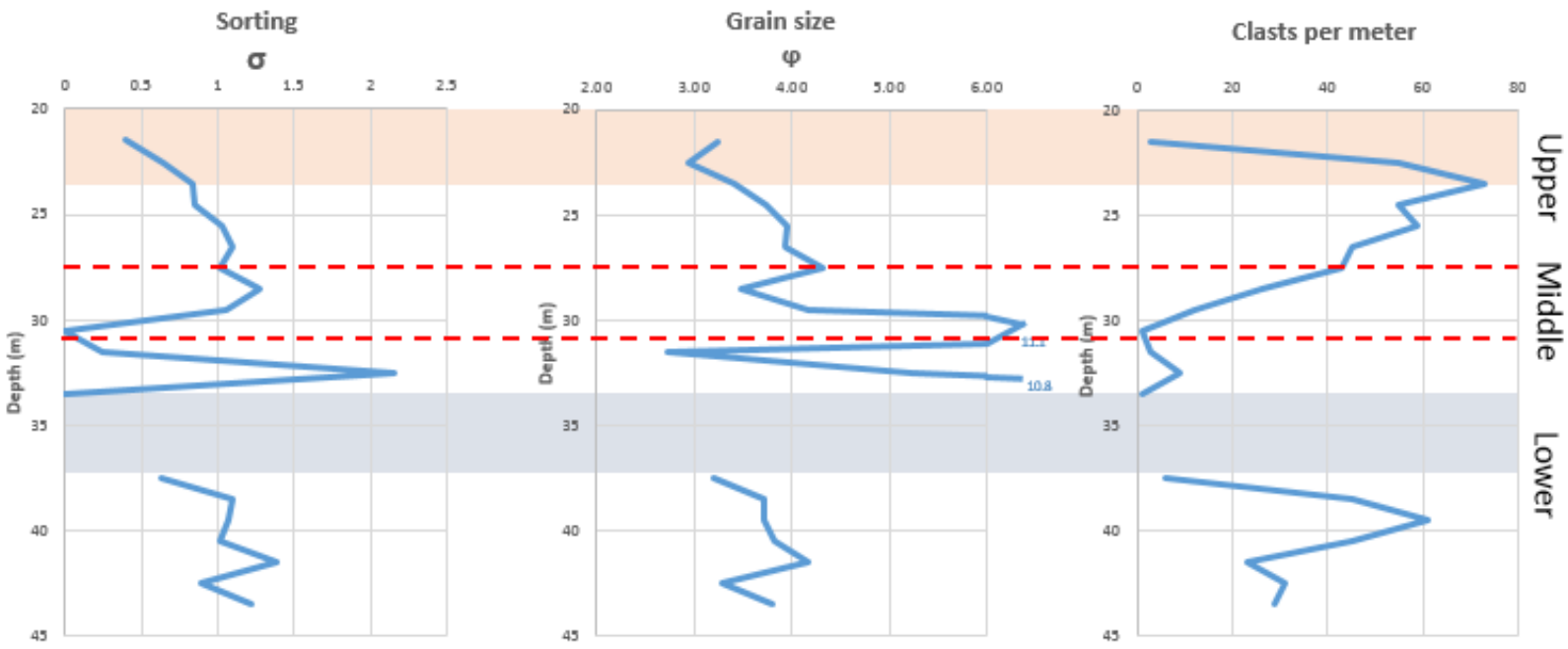


Figure 8. FC67-3 drill core, plots of key statistics versus depth in drill core. Upper, middle, and lower parts of the crater-filling unit are discussed in the text. Red shaded area indicates the portion where values are strongly affected by the 5-mm grain-size cut-off.

drill core shows the same discernable pattern of lower, middle, and upper parts as in the other drill core's crater-filling sequence. Drill core 67-3 has one missing core box, which results in drill-core loss from 33.9 to 37.6 m, a section within the lower part of the crater-filling sequence.

The lower part ranges from 43.9 to 30.5 m, and therefore is thicker than the comparable lower part in drill core 77-3. Number of clasts per meter rises substantially below the core-loss zone, but above the core loss, not so much. Sorting increases slightly below the core-loss zone, but above that zone there are strong fluctuations, which are likely a consequence of the relatively few clasts per meter in this interval (33.5-30.5 m). In the lower part, grain size is relatively coarse, and is very coarse ($\phi \sim 11$) in two places: above the core-loss zone and low in the middle part of the sequence.

The middle part, ranging from 30.5 to 27.5 m, is thinner in this drill core than in FC77-3. The fluctuating grain sizes and sorting continues from the part below, however, this fluctuation decreases towards the top of the interval. The number of clasts per meter increases upward within this part, which follows an upward reduction of the matrix content. This middle part shows some more stable trends in sorting, that increases steadily from $\sigma_\phi \sim 1.1$ to $< 0.5$ (poorly sorted to well sorted), and in grain size that falls off from $\phi \sim 4.3$ to $\sim 2.9$.

The increase in number of clasts continues into the upper part (from depths of 27.5 to 21.5 m), until the 5-mm cut-off size begins to affect the data (at a depth of 22.5 m). In the interval from 21.5 m to the top of the finer grained (calcarenite and calcisiltite) capping unit of the crater-moat fill (15.8 m), grain sizes are entirely below the cut-off size. But, we noted that the grains comprising the capping unit were well sorted and continuously size-graded (fining upward to the transitional contact with the overlying post-impact deposit, the Chattanooga Shale).

## DISCUSSION

In describing the conditions during formation and modification of Flynn Creek impact structure, Roddy (1968) noted the evident effects of the marine target environment, including erosion of the crater rim, scouring and removal of the surrounding ejecta blanket, and formation of a bedded (water-laid) breccia. Roddy (1968) described a lower breccia that underlies the bedded breccia, which he did not attribute entirely to aqueous deposition during the return of sea water. In subsequent studies of several marine-target impact craters, Ormö and Lindström (2000) noted that graded, bedded breccias including their fine-grained capping deposits (calcarentite and calcisiltite) were the consequence of the return flow of sea water into the impact structure during the early modification phase. In a recent review of marine impacts, Azad et al. (2015) also noted that breccias and bedded breccias are common in most marine impact structures.

Marine impact structures wherein line-logging data have been presented and that lend themselves well to comparison with our data and results are Lockne crater (~ 7.5 km diameter; Ordovician; Sweden), Tvären crater (~ 2 km in diameter; Ordovician; Sweden), and Chesapeake Bay impact structure (CBIS) (~ 40/85 km in diameter; Eocene; Virginia USA). The two given diameters for the CBIS are stated because the originally fresh 40 km wide crater rapidly expanded by extensive block slumping of a thick, poorly consolidated upper sedimentary target layer and thus formed a much larger modified crater (Horton et al. 2006 and references therein). However, because it is the formation of the 85-km wide crater that came to influence the resurge deposition, we here use the morphological crater with this diameter in our comparisons with Flynn Creek. The crater moat-filling breccias of relevance to this study that can be found within these craters have been studied by Ormö et al. (2007; Lockne and Tvären), Ormö et al. (2009;

Chesapeake Bay) and Sturkell et al. (2013; Lockne). The inferred water depth for Lockne and Tvären craters, 100 m or more (Ormö et al., 2007) is much deeper than the suggested target water depth at Flynn Creek (Roddy, 1968; Schieber and Over, 2005), which has been estimated at only about 10 m or so. The target water depth must then also be put in relation with the size of the crater (cf. Ormö et al., 2009). The shelf sea at the CBIS had an estimated water depth of a few tens of meters on its shoreward western side and was possibly as deep as ~300 m on its oceanic eastern side (Horton et al., 2005). The vertical trends or patterns in sorting, grain size, and clasts per meter for these three example marine-target craters are here compared to Flynn Creek's results in order to make inferences about origin of observed changes. Likewise, the putative resurge deposits in the interior of the ~ 5 km wide Wetumpka impact structure can give valuable hints in the interpretations as a reference for the nature of the deposits from an impact into very shallow relative target water depth. King and Ormö (2011) describe the target water depth at Wetumpka to have been less than a few tens of meters, which in combination with a poorly consolidated sedimentary target caused relatively thin and poorly sorted debris flow-like deposits in low terrain between slump blocks.

The Flynn Creek crater-moat breccias in both drill cores FC77-3 and FC67-3 show similar patterns in the sorting, grain size, and number of clasts per meter. Therefore, they will be discussed together in this section. Specifically, there are three parts to the crater moat-filling sequence in each drill core: a lower part that is a chaotic, matrix-supported unit; an upper part that is relatively well-sorted, normally graded, and generally clast-supported; and a middle part that represents a mixed version of the lower and upper parts. A remarkably similar sequence, but on a much larger scale, is described from CBIS where a lower slump breccia occurs below a zone of mixing (i.e., resurge occurring simultaneously with slumping), which is in turn overlain

– with a rather abrupt transition – by a better sorted and graded resurge breccia (Ormö et al. 2009). At Lockne, drill core Lockne-2 (also referred to as LOC02) is located in the inferred deepest part of the crater with the most complete infill sequence. Sturkell et al. (2013) presented a detailed description of this sequence, which they obtained by combining (1) published data from Ormö et al. (2010) on the transition to secular sediments at the top of the infill sequence, (2) data from Ormö et al. (2007) on the resurge deposits that follows below, (3) and their own new data for slump and rock avalanche breccias in the lower part of the CBIS Eyreville-A drill core.

Sturkell et al. (2013) showed that the slump deposits, below the resurge deposits in Lockne crater, are essentially matrix-supported, unsorted deposits. After an abrupt transition from the slump deposits, the resurge deposits show relatively good sorting which continue to improve upwards in concert with a generally fining-upwards trend through the over 120-m thick bed. This granulometric signature is typical for a forceful single resurge event rather than sets of several flows that might be expected at a shallow-water target.

Regarding Lockne and Tvären, when breaking down the granulometric data for the resurge deposits, Ormö et al. (2007) noted more subtle variations that can be linked to various phases of the resurge flow. Because Lockne had target water depth of over 500 m (see Lindström et al., 2005), the resurge there was forceful enough to generate a central water plume that subsequently collapsed and led to an outwards movement, or anti-resurge. This is, however, not the trend at Tvären, which formed in relatively shallower water (i.e., ~ 100 m). At Tvären, the resurge was forceful enough (like Lockne) to form a single graded bed, but not to generate any central water plume and subsequent anti-resurge. The Tvären core is not long enough to sufficiently penetrate the slump deposits below the resurge deposits to allow a similar analysis of

those breccias as for Lockne-2. In their line-logging of the crater moat infill of the CBIS, Ormö et al. (2009) noted two main units: a lower unit consisting of 77 m of coarse breccia (clast sizes ranging from $\phi \sim 4$ to ~ 11), which had poor sorting ($\sigma_\phi$ as high as ~ 2.0) and widely varying counts of clasts per meter. This unit was interpreted by Ormö et al. (2009) as a breccia deposit of mainly slumped material. The upper unit, ~ 93 m thick, consisted of finer breccia that is sub-divided into two parts. The lower part of the upper unit is a general coarsening upward sequence, wherein grain sizes increase gradually from $\phi \sim 4.0$ to ~ 5.0 over a span of about 50 m, but in that span, there were several very coarse intervals ($\phi \sim 11$) that represent departures from the gradual trend. The upper part of the upper unit is a general fining upward sequence of about 43 m wherein grain sizes decrease from $\phi \sim 4.0$ to ~ 2.0 and sorting is better (but still poor) at ~ 1.5. Sorting trends generally follow grain size rather closely in this upper part. Altogether the upper unit at CBIS is by Ormö et al. (2009) interpreted as the resurge sequence. However, the very low amount of clasts per meter (~8), generally poor sorting, and the reverse grading in the lower half lead them to suggest that the resurge to great extent was in the form of a debris flow due to high sediment content despite the relatively deep water. The normally graded upper part, albeit with high matrix content, is typical for hyperconcentrated flows (Costa 1988). Despite the significant differences in scale of the two structures, we suggest that Flynn Creek shows more similarities to CBIS than Lockne and Tvären. Especially, there are some noteworthy similarities in the two crater moat-filling breccia sequences. The lower unit at Chesapeake Bay, as described by Ormö et al. (2009), compares favorably in several ways to the lower part of the crater-moat breccia at Flynn Creek. In addition to the grain-size trend comparison and abrupt coarsening (up to ~ 11 $\phi$) in some narrow intervals, the overall poor sorting and wide variations in clasts per meter are similar in both instances. The upper unit at Chesapeake Bay, as described by Ormö et

al. (2009), is subdivided into a lower and upper section. The lower section compares favorably in several ways to the middle part of the Flynn Creek crater-moat breccia and the upper section compares favorably in several ways to the upper part of the Flynn Creek breccia. These comparisons include grain sizes, sorting values, and clasts per meter variations. Table 1 summarizes the comparison between Flynn Creek drill cores studied herein and Chesapeake Bay's Eyreville-A drill core.

At Flynn Creek, especially in the more complete FC77-3 core, we suggest that the lower part very much resembles the granulometric curves for the slump deposits at CBIS and Lockne. The middle and upper part of the FC77-3 core show comparable features with the resurge deposits of CBIS, and to some extent Lockne. The degree of sorting shows more of the upwards improvement noted at Lockne and Tvären, but in absolute values it lies closer to the poorer sorting observed at CBIS. There is also a less noticeable fining-up trend at Flynn Creek than at Lockne and Tvären, and again Flynn Creek seems to resemble more the complex situation noted at CBIS. Altogether, this could indicate a relatively shallow target water depth unable to generate a resurge flow of the strength seen at Lockne and Tvären, and possible more resembling the situation at CBIS with a flow affected by a relatively high amount of debris relative to the amount of available water (cf. Ormö et al. 2009).

There are some differences between the two Flynn Creek drill cores 77-3 and 67-3, as described in the results section. For example, the drill core FC77-3 exhibits one interval of very coarse debris, whereas drill core FC67-3 apparently has two closely spaced coarse intervals. These coarse intervals are interpreted as slump deposits from the central uplift, as this was closer to the drill sites than to the crater rim. These coarse clasts may have derived from an episode of central-peak collapse just as resurge was starting to move into the moat area (cf.

coarse intervals of breccia within the crater-moat sequence in both Lockne and Chesapeake Bay; Ormö et al., 2007; 2009). Another difference is the disparate thickness of three parts of the crater-moat breccia in drill core FC77-3 versus FC67-3. These differences may be due to slight differences in distance from the rim and central uplift or to asymmetry of resurge flow (cf. Lockne-1 versus Lockne-2 cores, as described in Ormö et al., 2007). Table 2 summarizes these differences and their possible origins at Flynn Creek.

The vertical distribution of clast types (dolostone and limestone) is not random and is different in drill core FC77-3 versus FC67-3 (Figures 5 and 6). It should be noted that limestone clasts occur with approximately the same frequency in both drill cores (7% and 6%, respectively). However, in drill core FC77-3, limestone clasts more commonly appear within the upper third of the upper part of the crater-moat breccia (i.e., within the graded resurge deposit).

In contrast, within drill core FC67-3, limestone clasts appear more commonly in the lower two-thirds of the lower part and in the upper part (but not in the middle part) of the crater-moat breccia. This apparent absence from the middle part is not easy to explain, but the apparent absence of limestone clasts from the upper third of the lower part may be due to the combined effect of missing core pieces and the presence of some large clasts in this interval. We interpret the unequal distribution of limestone clasts between the two Flynn Creek drill cores as an effect of differential provenance of clasts. We suggest that limestone particles within the crater-moat breccia in FC67-3 may have come from a different source than FC77-3, one with more limestone beds within it. The stratigraphic section at Flynn Creek was described by Conant and Swanson (1961) and Wilson (1962). Roddy (1968) reviewed this stratigraphy and pointed out that the formal stratigraphic units in the area consist of varying mixtures of dolostone and limestone.

Table 1. Comparison of two drill cores from Flynn Creek impact structure, discussed in this paper, and Chesapeake Bay, Eyreville-A drill core.

<table>
<tr><th>Flynn Creek - FC67-3</th><th>Flynn Creek - FC77-3</th><th colspan="2">Chesapeake Bay-Eyreville A</th></tr>
<tr><td>Upper part: fining upward (φ around 2.8-4.3 improvement of the sorting (σ around 0.3-1.1), ), drastic increase in number of clasts per meter.</td><td>Upper part: fining upward (φ around 2.9-4.5), improvement of the sorting (σ around 0.7-1.3), drastic increase in number of clasts per meter.</td><td rowspan="2">Upper part</td><td>Upper section: fining upward (φ around 2.1-5), improvement of the sorting (σ around 0.5-1.5), increase in number of clasts per meter.</td></tr>
<tr><td>Middle part: grain size fluctuations (φ around 3.-4.5) , reduction in matrix content (σ around 0.7-1.5), increased number of clasts per meter.</td><td>Middle part: grain size fluctuations (φ around 3.5-11.7), reduction in matrix content (σ around 1.1-1.3), increased number of clasts per meter.</td><td>Lower section: grain size fluctuations (φ around 2.5-11) reduction in matrix content (σ around 0.9-2.2), number of clasts per meter decreases upward.</td></tr>
<tr><td>Lower part: abrupt coarsening upward with φ values reaching 10.8 in narrow intervals at ~ 33 meter depth, poor sorting (σ around 0.6-2.2), wide variation in number of clasts per meter.</td><td>Lower part: abrupt coarsening upward with φ values reaching 11.7 in narrow intervals at ~ 30 meter depth, poor sorting (σ around 0.7-1.5), wide variation in number of clasts per meter.</td><td colspan="2">Lower part: abrupt coarsening upward with φ values reaching ~ 11 in narrow intervals at different depths, poor sorting (σ ~ 1.5), wide variation in number of clasts per meter.</td></tr>
</table>

Table 2. Comparison of three parts of each of two drill cores from Flynn Creek impact structure, studied herein, and the suggested genesis of each part.

| FC77-3 | FC67-3 |
|---|---|
| Upper part: resurge deposits with thickness of 10.1 meters | Upper part: resurge deposits with thickness of 11.7 meters |
| Middle part: mixture of resurge and slump deposits with thickness of 11 meters | Middle part: mixture of resurge and slump deposits with thickness of 3 meters. Large block (φ = 11.1) at 30 meter depth |
| Lower part: slump deposits with thickness of 6 meters. Coarse deposits (φ = 11.7) at ~ 30 m depth. TOTAL thickness = 27.1 meters | Lower part: slump deposits with thickness of 13.4 meters. Coarse deposits (φ = 10.8) at ~ 33 m depth. TOTAL thickness = 28.1 meters |

The only formation that is entirely limestone is the Cannon Limestone, which is the lowermost formation in the Nashville Group. Above the Cannon lies the Catheys-Leipers Formation, a unit that has much less limestone content according to Roddy (1968). If this observation about limestone content is pertinent, a point source on the crater rim where Cannon Limestone could have been eroded during resurge may have been a more significant source for breccia particles in the area of drill core FC67-3 versus FC77-3. Until more is known about the conditions of impact (both impactor and target), the significance of this observation may not be clear.

Regarding the "breccia-in-breccia" (intraformational) clasts noted above, we interpret these as coming from fall-back deposits on the top of central-uplift area, being reworked and incorporated into the crater moat deposit due to erosion and redeposition by slumping (cf. Ormö

et al., 2007). We suggest that these slumping "breccia-in-breccia" clasts may have been from central uplift area instead crater rim considering the proximity between drill cores and crater center but it does not exclude a rim provenience.

The early modification stage of formation of Flynn Creek impact structure can be divided into sub-stages, which we think likely correspond to the textural sequence in the crater moat-filling breccia in both drill cores examined in the present study. Figure 9 shows the interpreted sequence of events during Flynn Creek crater formation, including fall-back (step 1), slumping from crater rim/central uplift during early central-peak formation (step 2), central-peak collapse and associated slumping of coarse blocks (step 3), initial stage of marine resurge (slump and resurge mixing; step 4), and resurge sedimentation (step 5), which is then followed by waning water energy and secular deposition (step 5). In the crater moat-filling breccia sequence described in the present paper, step 1, 2, and 3, corresponds to the lower part of the breccia, which is lying upon sub-crater rocks. Step 3 corresponds to the coarse layer(s) at the top of the lower breccia (i.e., the ~ $\phi$ 11 clasts in FC77-3). The middle part of the breccia corresponds to a transition between steps 3 and 4, and step 4 corresponds to the upper part of the breccia (i.e., resurge deposits). Step 5 corresponds to secular sedimentation, represented by the post-impact Chattanooga Shale.

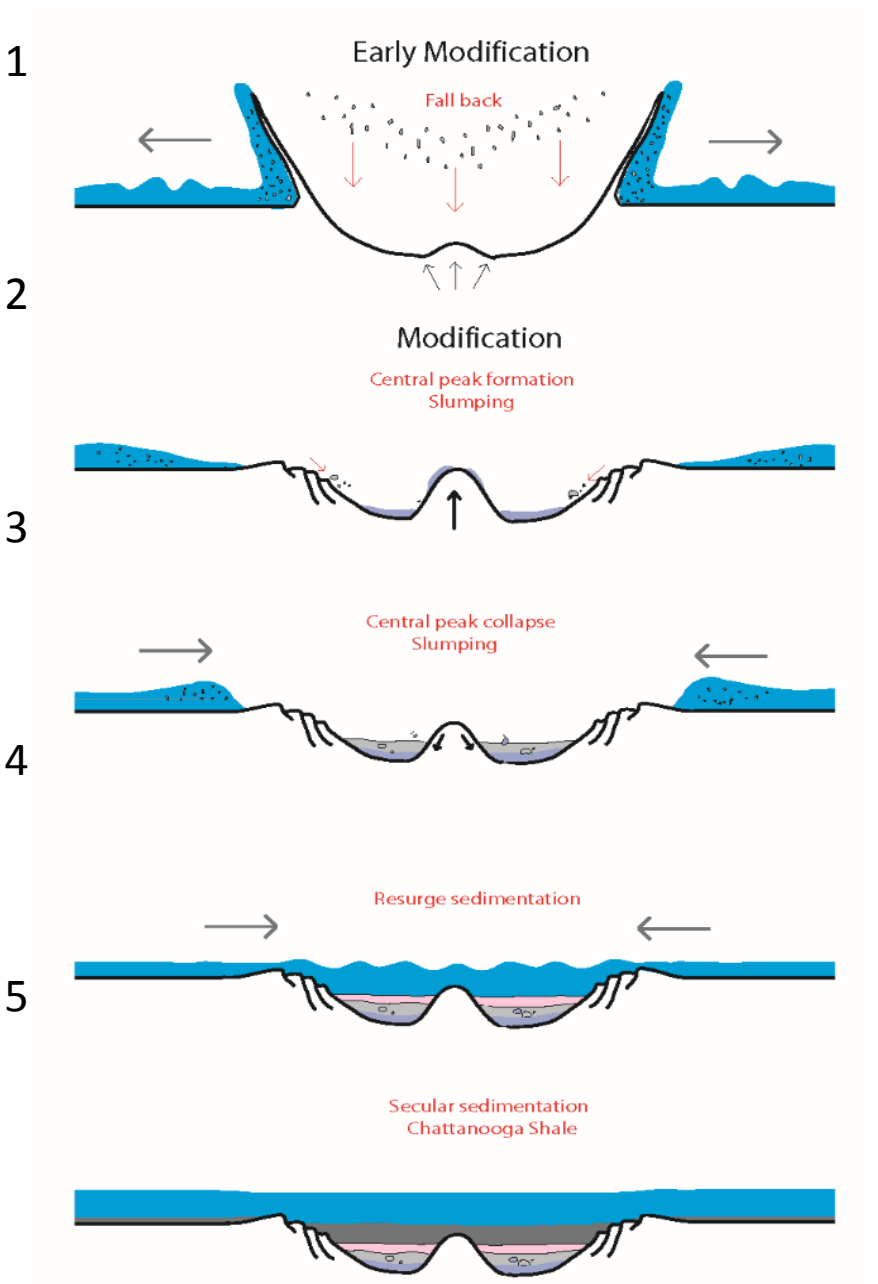


Figure 9. Sequence of events and process diagram showing stages in development of Flynn Creek impact structure as envisioned in this paper. Steps 1-5 are discussed in the text. Steps 1-2 is related to deposition of the lower part of the crater-filling breccia unit. Steps 2-3 relates to the middle part, and steps 3-4 to the resurge (upper) part. Step 5 is post-impact deposition (Chattanooga Shale).

## CONCLUSIONS

Flynn Creek impact structure contains a crater moat-filling breccia sequence that is approximately 27-m thick in both of the two drill cores studied herein, specifically FC77-3 (in the northeastern quadrant) and FC67-3 (in the southeastern quadrant). Both drill cores exhibit a three-part sequence within the crater moat-filling breccia. The lower part, a non-bedded slump-related breccia, is coarse-grained and poorly sorted. In one or two narrow intervals near the top of the lower part of both cores, there are very large clasts, which may have been derived from a collapse event in the central peak. The middle part, which is slightly less coarse and has variable sorting, is a deposit that is a transition between slumping and marine resurge. In the upper part, a graded resurge breccia formed by the resurge proper, grain sizes are finer and sorting is better. The uppermost part of the sequence is a capping unit composed of fine-grained calcarenite and calcisilite deposits. There is a distinctive contact with the overlying post-impact unit, the Chattanooga Shale. Parts of the crater moat-filling breccia described herein correspond to separate steps in the early modification stage at Flynn Creek, including slumping, central peak collapse, resurge sedimentation, and secular sedimentation.

Flynn Creek's crater moat-filling breccia sequence has many important similarities with breccia sequences of two well-documented Paleozoic marine craters, Lockne (~ 7.5 km) and Tvären (~ 2 km), and the larger Eocene marine impact structure, Chesapeake Bay (~ 40/85 km), whereas it differs from the debris flow-like resurge deposits reported from the shallow water Wetumpka impact crater (cf. King et al., 2006). In particular, there are similar patterns of grain size, sorting, and clasts per meter counts in the comparable parts of the crater moat-filling breccias of the former craters, which include lower, middle, and upper sub-divisions as at Flynn Creek. All in all, the granulometric analysis and comparisons with the equivalent deposits at

other marine target craters with known target water depths allow the assumption that the target water depth for Flynn Creek would have been at least as deep as the hitherto suggested 10 m.

The distribution of minority limestone clasts within the dominant dolostone clast population of the Flynn Creek crater moat-filling breccia suggests an asymmetry of provenance for those particles that may relate to as yet unknown effects of the impact environment, including target stratigraphy exposures on the initial crater rim.

## ACKNOWLEDGEMENTS

We thank the National Aeronautics and Space Administration, Planetary Geology and Geophysics Program, for supporting the project proposal by J. J. Hagerty and others (NASA PGG NNH14AY73I), of which this publication is a partial result. We also thank the Astrogeology Branch of the U.S. Geological Survey in Flagstaff, Arizona, for organizing the Flynn Creek drill-core collection, hosting our visit to work on these materials, and providing many forms of assistance in sampling. The first author thanks the Barringer Family Fund for Meteorite Crater Research for partial support of this work. The work by J. Ormö has been partially supported by grants AYA2008-03467/ESP, AYA2011-24780/ESP, AYA2012-39362-C02-01, ESP2014-59789-P, ESP2017-87676-C5-1-R and ESP2015-65712-C5-1-R from the Spanish Ministry of Economy and Competitiveness and Fondo Europeo de Desarrollo Regional.

## REFERENCES

Azad, A. S., Dypvik, H., and Kalleson, E. 2015. Sedimentation in marine impact craters – Insight from the Ritland impact structure. *Sedimentary Geology* 318:97-112.

Conant, L.C. and Swanson, V. E. 1961. Chattanooga Shale and related rocks of central

Tennessee and nearby areas. U. S. Geological Survey Professional Paper 357, 88p.

Costa, J.E., 1988. Rheologic, geomorphic, and sedimentologic differentiation of water floods, hyperconcentrated flows, and debris flows, *in* Baker, V.R., Kochel, R.C., and Patten, P.C. (eds) Flood Geomorphology: Wiley-Intersciences, New York, p. 113-122

Evenick, J. C., and Hatcher, R. D., Jr. 2007. Geologic map and cross sections of the Flynn Creek impact structure, Tennessee. GSA Map and Chart Series 95. Boulder, Colorado. Geological Society of America. 1:12,000.

Folk, R. L. 1974. *The petrology of sedimentary rocks*. Austin, Texas. Hemphill's. 183p.

French, B. M., and Short, N. M., 1968. Shock metamorphism of natural materials: Baltimore, Mono Book Corp., 644 p.

Gaither, T. A., Hagerty, J. J., and Bailen, M. 2015. The USGS Flynn Creek crater drill core collection: progress on a web-based portal and online database for the planetary science community (abstract #2089). 46th Lunar and Planetary Science Conference.

Hagerty, J. J., HcHone, J. F., and Gaither, T. A. 2013. The Flynn Creek crater drill core collection at the USGS in Flagstaff, Arizona (abstract #2122). 47th Lunar and Planetary Science Conference.

Horton Jr. J. W., Powars D. S., and Gohn G. S. 2005. Studies of the Chesapeake Bay impact structure-Introduction and discussion. In Studies of the Chesapeake Bay impact structure – the USGS-NASA Langley corehole, Hampton, Virginia, and related coreholes and geophysical surveys, edited by Horton Jr. J. W., Powars D. S., and Gohn G. S., U. S. Geological Survey Professional Paper 1688.

Horton Jr. W. J., Ormö J., Powars D. S., and Gohn G. S. 2006. Chesapeake Bay impact structure: Morphology, crater fill, and relevance for impact processes on Mars. Meteoritics and

Planetary Science 41: 1613–1624.

Lindström, M., Shuvalov, V., and Ivanov, B., 2005. Lockne crater as a result of marine-target oblique impact: *Planetary and Space Science*, 53:803-815.

King, D. T., Jr., Adrian, D. R., Ormö, J., Petruny, L. W., Hagerty, J. J., Gaither, T. A., and Jaret, S. J. 2015. Flynn Creek impact structure, Tennessee: its crater-filling breccia in comparison to two other small Paleozoic impact structures and their breccia units (abstract #260475). *GSA Abstracts with Programs* 47.

King, D. T., Jr. and J. Ormö, 2011. Wetumpka – a marine target impact structure examined in the field and by shallow core drilling, in Garry, W.B., and J.E. Bleacher, eds., *Analogues for planetary exploration*: Boulder, Colorado, Geological Society of America, Special Paper 483, p. 287-300.

King, D. T., Jr., J. Ormö, L. W. Petruny, and T. L. Neathery 2006. Role of sea water in the formation of the Late Cretaceous Wetumpka impact structure, inner Gulf Coastal Plain of Alabama, USA. *Meteoritics and Planetary Science*, 41:1625-1631.

Mazzullo, J. M., Meyer, A., and Kidd, R. B., 1988. New sediment classification scheme for the Ocean Drilling Program. In Mazzullo, J. M., and Graham, A.G. (Eds.), Handbook for shipboard sedimentologists. ODP Tech. Note, 8:45–67Ormö, J. and Lindström, M. 2000. When a cosmic impact strikes the seabed. *Geological Magazine* 137:67-80.

Ormö, J. and Lindström, M. 2000. When a cosmic impact strikes the seabed. *Geological Magazine* 137:67-80.

Ormö, J., Sturkell, E., Lindström, M. 2007. Sedimentological analysis of resurge deposits at the Lockne and Tvären craters: clues to flow dynamics. *Meteoritics and Planetary Science* 42:1929-1943.

Ormö, J., Sturkell, E., Horton, J.W., Jr., Powars, D.S., and Edwards, L.E. 2009. Comparison of clast frequency and size in the Exmore sediment-clast breccia, Eyreville and Langley cores, Chesapeake Bay impact structure: clues to the resurge process. Edited by Gohn, G. S., Koeberl, C., Miller, K. G., and Reimold, W.U. *The ICDP-USGS deep drilling project in the Chesapeake Bay impact structure: results from the Eyreville coreholes*. Boulder, Colorado. Geological Society of America Special Paper 458, pp. 617-632.

Osinski. G.R., Grieve, R.A.F., Chanou, A., and Sapers, H.M., 2016. The suevite conundrum, part 1: The Ries suevite and Sudbury Onaping Formation compared: *Meteoritics & Planetary Science*, v.51, p. 2316-2333.

Roddy, D. J. 1966. The Paleozoic crater at Flynn Creek, Tennessee [dissertation]. Pasadena, California. California Institute of Technology. 232p.

Roddy, D. J. 1968. The Flynn Creek crater, Tennessee. Edited by French, B. M., and Short, N. M. *Shock and Metamorphism of Natural Materials*. Baltimore, Maryland. Mono Book Corporation. pp. 291–322.

Roddy, D. J. 1979. Structural deformation at the Flynn Creek impact crater, Tennessee: a preliminary report on deep drilling. *Lunar and Planetary Science* 10:2519-2534.

Schieber, J. and Over, J. D. 2005. Sedimentary fill of the Late Devonian Flynn Creek crater: a hard target marine impact. Edited by Over, D. J., Morrow, J. R., and Wignall, P. B. *Understanding Late Devonian and Permian-Triassic Biotic and Climatic Events: Towards and Integrated Approach*. New York. Elsevier. pp. 51-69.

Roddy D. J. 1980. Completion of a Deep Drilling Program at the Flynn Creek Impact Crater, Tennessee (abstract #1335). *11th Lunar and Planetary Science Conference*.

Sturkell, E., Ormö, J., and Lepinette, A. 2013. Early modification stage (pre-resurge) sediment

mobilization in the Lockne concentric, marine-target crater, Sweden. *Meteoritics and Planetary Science* 48:321-338.

Wilson Jr. C. W. 1962. Stratigraphy and geologicc history of Middle Ordovician rocks of central Tennessee. *Bulletin of the Geological Society of America* 73:481-504.

## CHAPTER 2

# Petrographic characteristics of crater moat-filling breccia, Flynn Creek impact structure, Tennessee.

L. De Marchi, D. T. King, Jr., W. E. Hames, and J. Ormö

[1]Deptartment of Geosciences, Auburn University, Auburn, Alabama 36849

[2]Centro de Astrobiología (INTA-CSIC), Madrid, Spain

**Abstract -** Petrographic study of thin sections including microprobe analyses shows that the Flynn Creek crater moat-filling breccia sequence (i.e., the fall-back, slumping, and resurge deposits) has distinctive fine-scale compositional characteristics regarding fossils, chalcedony, quartz grains, and melt particles. Regarding Flynn Creek's melt particles, aqueous resurge deposits contain two types of melt: a previously known grey silica melt and a previously unknown phosphatic amber-colored melt particles. The amber melt co-occurs with grains of chalcedony and fossils containing chalcedony, plus some quartz sand and granules, all of which likely originated in a mineralogically distinctive bed at the base of the Chattanooga Shale. Uneven distribution of petrographic components from the crater moat on opposite sides of the crater moat suggests possible ejecta asymmetry preserved within the resurge deposits of the crater moat.

## INTRODUCTION

The Flynn Creek impact structure is a marine-target crater formed approximately 382 million years ago (during Late Devonian) on the northeastern edge of the central basin of Tennessee (Roddy, 1968; Scheiber and Over, 2005; Adrian et al., 2018). Located in Jackson County near the town of Cookeville, this well-known impact crater is exposed at the surface and has been relatively extensively drilled as compared to other impact structures. Figure 10 shows the location and geology of the Flynn Creek impact structure, and the impact-affected stratigraphic section.

The Flynn Creek impact event occurred in an epicontinental shelf setting in shallow marine waters that covered eroded, Upper Ordovician flat-lying carbonates ranging from the Knox Group through the Catheys-Leipers Formation (Fig. 10). Atop these Upper Ordovician formations and lying upon the regional unconformity truncating them, is the Chattanooga Shale, which was just beginning to be deposited across the area at the time of impact (Scheiber and Over, 2005, Adrian et al., 2018). We think that only a few meters at most of the Chattanooga existed at the time of impact, and this interpretation is supported by the findings of Adrian et al. (2018; in review).

The impact produced a ~3.8 km, irregularly shaped, complex crater that excavated to a depth of approximately 150 m within the carbonate target rocks (Conant and Swanson, 1961; Roddy, 1968). Below the crater, impact compression deformed underlying strata up to a depth of 500 m or perhaps slightly more (King et al., 2018), and upon inward material displacement during crater modification, formed a central uplift. After the impact, the structure was filled by fall-back materials, slump deposits, and resurge sediments, as noted by De Marchi et al. (2018; in review) and the present report. The aqueous resurge deposits contained substantial proximal

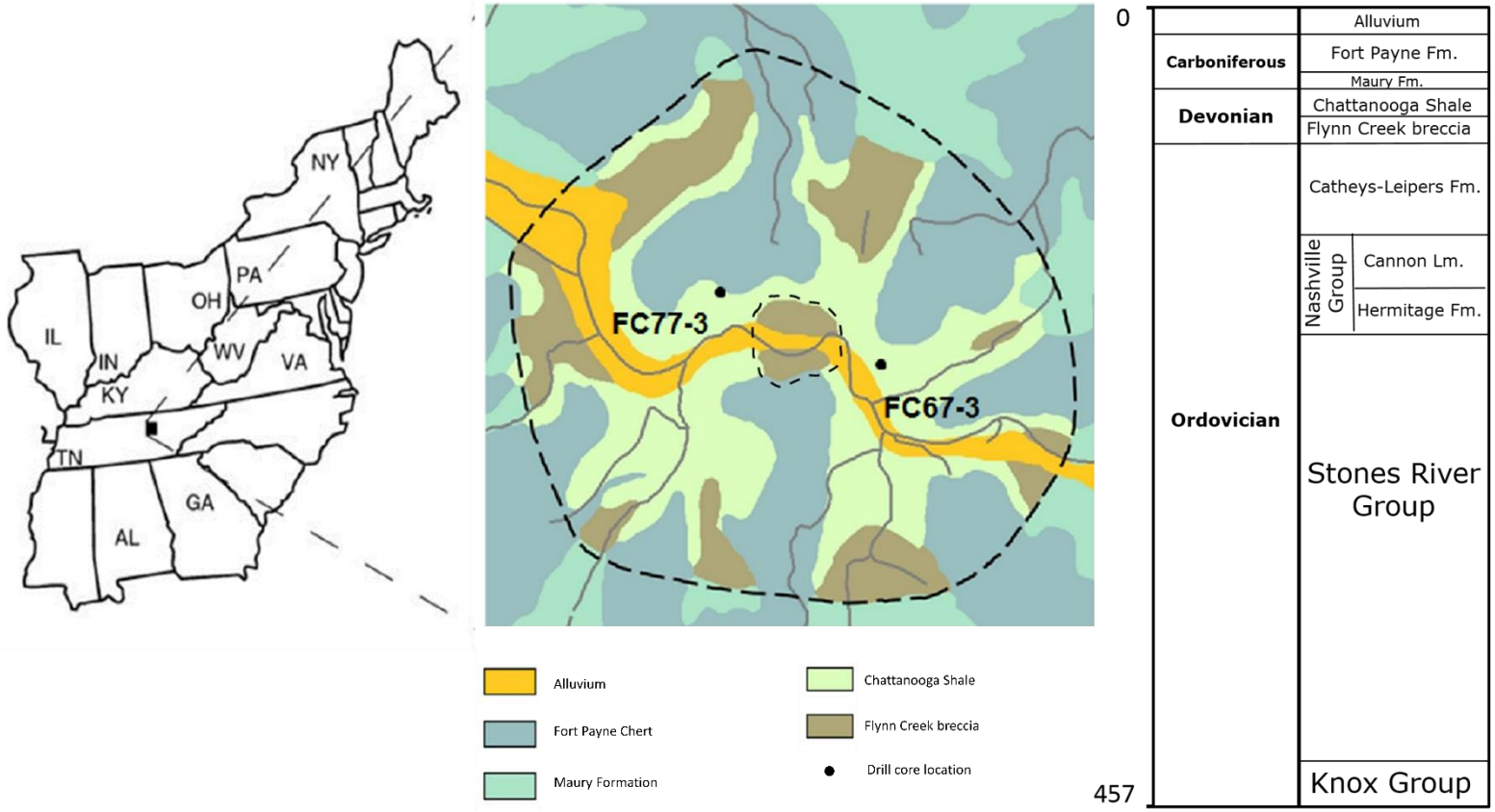


Figure 10. Geological map of Flynn Creek impact structure (adapted from U.S. Geological Survey, 2017), showing the location of the two drill cores used in the present study. Interpreted limit of outer rim (dashed line) is from Roddy (1968); limit of central uplift, which is capped by Flynn Creek impact breccia is from Adrian et al. (2017). At right: Local stratigraphic columnar section of the Flynn Creek target area (adapted from Roddy, 1968). Stratigraphic depth of the informal Flynn Creek breccia varies and is shown schematically here.

ejecta material that was transported back into the crater by the energetic return flow of displaced water mass (De Marchi et al., 2018; in review). The crater-moat filling breccias and central uplift breccias at Flynn Creek have an informal stratigraphic name – the Flynn Creek breccia – as shown on geologic maps of the impact structure (Roddy, 1990; Evenick and Hatcher, 2007; U.S. Geological Survey, 2017).

Crater-filling deposits are overlain by the Upper Devonian marine Chattanooga Shale, which displays a much thicker sequence (up to 70 m) within the crater, as compared to outside the structure, where deposits are, on average, approximately 10 m thick (Conant and Swanson, 1961; Scheiber and Over, 2005). Flynn Creek's sedimentary sequence was subsequently overlain by the Carboniferous Maury and Fort Payne formations. After a substantial episode of surficial erosion and phreatic karstic development, Quaternary alluvial deposits blanketed parts of the crater area (Fig 10).

Study of Flynn Creek that provided an initial proof of impact was initiated by David R. Roddy, a USGS geologist, as a doctoral study topic (Roddy, 1966). His main lines of evidence were shatter cones and the overall physical structure and distribution of impact breccias. After his doctoral program, a multi-year core-drilling campaign was conducted by the USGS under his direction, thus producing 18 individual drilled core holes. Later, three other non-USGS drill cores were added to Roddy's Flynn Creek collection. Eventually, the USGS Flynn Creek drill-core collection was transported to and warehoused at the USGS Astrogeology Center in Flagstaff, Arizona. At present, more than 2,000 standard core storage boxes hold these archived drill cores. This study is based on description and sampling of two of these USGS drill cores from the crater moat.

As suggested by recent studies of one other of these USGS drill cores (Adrian et al., 2018), and based on line-logging statistical analysis and direct observations of drill cores FC77-3 and FC67-3 (De Marchi et al., 2018; in review), it is evident that the Flynn Creek crater moat was filled in by a sequence of deposits – fall-back, slumping, and resurge sediments (in that order) – during the crater's early modification stage. Generally speaking, the fall-back and slumping produced a lower chaotic breccia unit (~ 16-17 m thick) and the marine resurge developed an overlying, normally graded breccia deposit of approximately 10-12 m thickness. In previous work, the lower chaotic breccia was referred to as the "non-bedded breccia" (Wilson and Roddy, 1990; Evenick, 2005) and the resurge breccia has been called the "bedded breccia" (Wilson and Roddy, 1990; Evenick, 2005).

Work by De Marchi et al. (2018; in review) has documented the characteristics of the crater-filling deposits at Flynn Creek (i.e., the "crater moat breccias"), which can be distinguished by careful study of granulometry, sorting, matrix content, and constituent grains. Figure 11 shows drill-core positions and depicts the four main subdivisions of the crater-filling sequence: (1) a thin layer of fall-back sediments at the bottom followed by (2) slump deposits, which are divided into a lower coarsening upward section, and an upper part with varying sizes and sorting. Then, this is overlain by (3) a better sorted, normally graded breccia unit formed by resurging water and a (4) fine-grained, laminated carbonate unit that grades upward into the post-impact deposits of the Chattanooga Shale (De Marchi et al., 2018; in review).

Previous work by Adrian et al. (2018; in review) and De Marchi et al. (2018; in review) predicted that the Chattanooga Shale was just beginning to be deposited at the time of impact, based on the minuscule shale clast content within the Flynn Creek breccia. Studies of the stratigraphy of the lower beds of the Chattanooga Shale have shown that there is a basal

conglomeratic zone that is rich in fossils, chalcedony (including fossils bearing chalcedony), quartz grains, and the amorphous phosphate mineral *collophane,* with color varying to amber-yellow to opaque brown or black (Smith and Whitlatch, 1940; Conant and Swanson, 1961). Locally called the "blue phosphate," this bed of weathered debris was derived mainly from the underlying Catheys-Leipers Formation and contains many of the ingredients of the ejecta-rich resurge deposits, as noted in this paper. This mineralogically distinctive basal Chattanooga bed is interpreted here to have been involved in producing equally distinctive ejecta, which ended up within the impact resurge deposits of the Flynn Creek crater moat, as described in this paper.

The present study follows on the drill-core line-logging and statistical analysis research by De Marchi et al. (2018; in review) and looks at these crater-filling units for the first time at petrographic scale. The main objective of the present study is a detailed petrographic investigation of thin sections, taken at selected spots throughout the crater-filling sequences in drill cores FC67-3 and FC77-3. These drill cores are on opposite sides of the central uplift and within the crater moat. The main focus of the present work is to characterize clasts below the megascopic line-logging cut-off size (5 mm) of our previous study, and explain how their properties and compositions relate to the crater-filling process at Flynn Creek in the crater moat. In the present study, we intensified the search for impact-related features such as impact-affected quartz grains and melt particles. Even though a convincingly large population of impact-affected quartz grains (especially those with well-developed planar deformation structures (PDFs) remains elusive at Flynn Creek, we report for the first time the co-occurrence of two types of melt particles at Flynn Creek (grey and amber-colored melts).

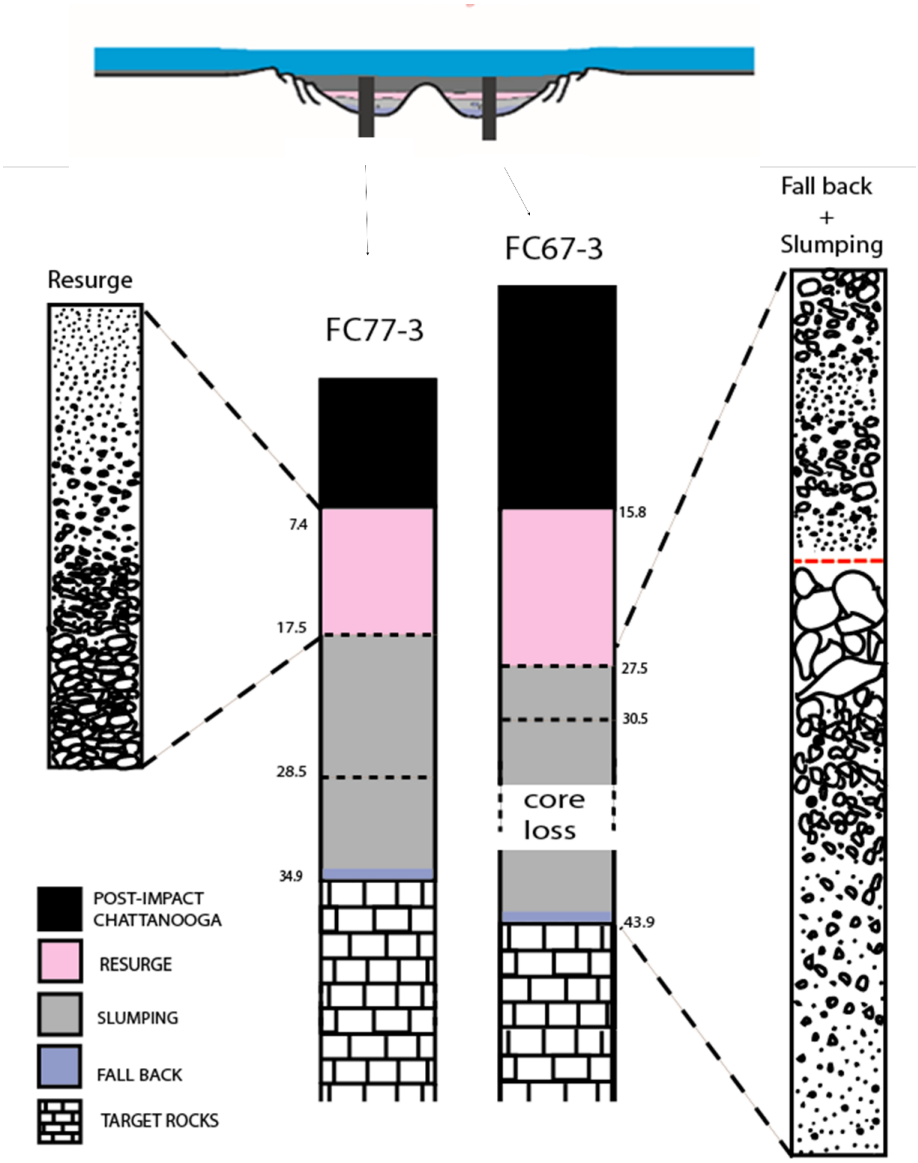


Figure 11. Inset at top: Schematic cross section of Flynn Creek impact structure, showing location of drill cores FC77-3 and FC67-3 on opposite sides of the central uplift. Below: Simplified core logs for FC77-3 and FC67-3, including schematic depictions of grain size changes for the resurge unit in FC77-3 and the fall-back and slump-deposited unit in FC67-3, adapted from core description and line-logging analysis by De Marchi et al. (2018; in review). Core logs show (from top down): post-impact Chattanooga Shale, resurge deposits, slump deposits, and fall back material, which are color-coded. In FC67-3 grain-size schematic, slumping is in two parts divided by the red dashed line. The lower slump deposit has a coarse interval at the top, which is attributed to possible central peak collapse (De Marchi et al., in review). Core logs are positioned relative to one another on the shale-breccia contact (datum). Scale in meters.

## METHODS

During examination of Flynn Creek crater drill core and high-resolution Flynn Creek core-box photographs, a total of 66 representative core samples were chosen for petrographic analysis from throughout the crater-filling deposits in both drill cores of this study. Of these 66 samples, 29 representative core samples were selected from drill core FC67-3 and 37 from drill core FC77-3. An additional 4 samples from within the lowermost layers of the overlying Chattanooga Shale were collected from drill core FC67-3. Thin sections of all 70 core samples were made by National Petrographic Service, Houston, and investigated using a standard petrographic microscope in order to describe rock textures, search for possible shock deformation features and to identify lithic constituents, which included various kinds of lithic clasts, fossil fragments, quartz and other silicate grains, and impact melt particles. During petrographic analysis, volume percentages of total matrix and sizes and volume percentages of individual non-matrix components were obtained. Petrographic data on size and shape of lithic clasts were also collected from each thin section. The lithology of the main types of carbonate clasts (dolostones and minor limestones) were classified according to Dunham (1962) as mudstone, wackestone, packstone, and grainstone for each grain. The clasts were mainly dolostone, but also there was some limestone, chert, and shale. Note was also made of the main types of fossils (e.g., brachiopods, etc.), petrographic types of quartz and other silicate grains, the granular characteristics and diagenetic occurrences of chalcedony, and the occurrence and granular characteristics of two types of melt particles. The estimates of content by volume were made using a standard visual comparison chart (Terry and Chilingarian, 1955).

From among the several uncovered and polished thin sections made for this study, three were selected for electron microprobe (EMP) study because they contain newly discovered melt

fragments. The instrument used was a JEOL-8600 electron microprobe, which is located in the Geosciences Department at Auburn University. Qualitative analyses, with beam operating conditions of 15 kV and 20nA, were based on back-scattered electron (BSE) and stage scan mapping, set up for rendering Ca, Mg, Fe, and Si images. Quantitative elemental analyses were also acquired at three different spots within the Si-rich melt fragment in order to obtain compositional information. Additional single-spot analyses on energy-dispersive spectrometry (EDS) mode were used for identification of elements not mapped on stage scan.

## RESULTS

By far, carbonate clasts were the main type of lithic component in the Flynn Creek crater-filling breccias. Carbonate clasts were mainly dolostones, which were mixed with minor limestones (6%). Figure 12 shows examples of the textural variation among carbonate clasts, which were classified as to inferred original texture according to Dunham (1962). In addition to carbonate clasts, the Flynn Creek breccias contained minor shale clasts (<0.5%), small and variable amounts of silicate grains (quartz - up to 6%; chert - up to 0.5%,\; and feldspar - up to 0.5%), and various types of fossil fragments (up to 12%). Figure 13 shows a petrographic view of a typical shale clast including fine quartz grains and fossil fragments.

Petrographic analysis of the fossil content within crater-filling breccias shows that fossils

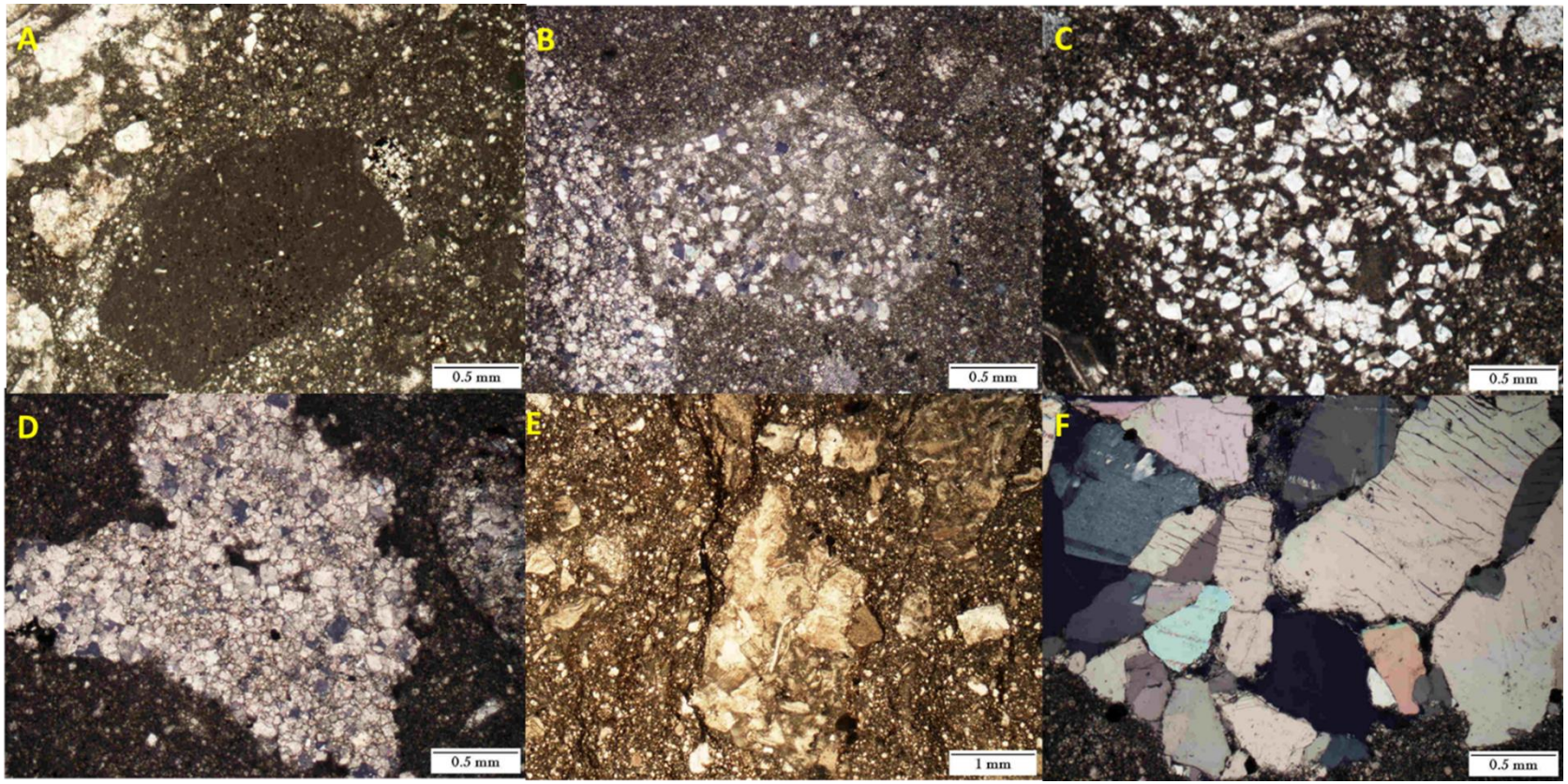


Figure 12. Representative photomicrographs of various constituent carbonate clasts within crater-filling deposits at Flynn Creek (interpreted original texture is classified according to Dunham, 1962). A: mudstone; B: wackestone; C: packstone; D: grainstone; E: grainstone with high fossil content; F: crystalline carbonate.

are mainly represented by fragments of brachiopod, echinoderm, bryozoan, trilobite, and coral. Figure 14 shows some representative examples of fossil fragments from the crater-filling breccias. Fossils tend to occur *within* carbonate clasts in the part of the crater-filling section that is close to the bottom of the deposit (fall-back and slump deposits), whereas fossils in the middle and upper parts of the crater-filling deposits more commonly occur as fossil-only clasts dispersed within the resurge breccia matrix.

Figure 15 shows graphs of the vertical trends in the volume percentage of each type of fossil and, at right in each instance, the total fossil content within drill cores. The drill cores have differences in vertical fossil dispersion as well. Data for drill core FC67-3 shows that all fossil types follow the same general vertical distribution as compared to one another and to the "total fossil" trend. These data confirm that most fossil-only clasts occur between 20 and 27 m depth and that the fossils within clasts are confined to the lower few meters where fossils are embedded within large carbonate clasts. In contrast, FC77-3 shows fossil content widely spread vertically throughout the breccia deposit, and an oscillating relative abundance curve that reflects fossils both as isolated grains and within carbonate clasts spanning the whole interval. There is a natural decreasing upwards trend in fossil content, which is likely caused by the overall decrease in grain size in the breccia. Eventually, fossil fragments became unrecognizable as they approach the size of associated matrix content.

In both drill cores, some fossil fragments (but not specific taxa) are associated with selective chalcedony replacement, which was also observed in the lower beds of the Chattanooga Shale (Smith and Whitlatch, 1940). Figure 16 shows an example of this diagenetic, selective-replacement phenomenon and the graphs therein show how closely associated the occurrence of chalcedony is with fossil content in the rocks.

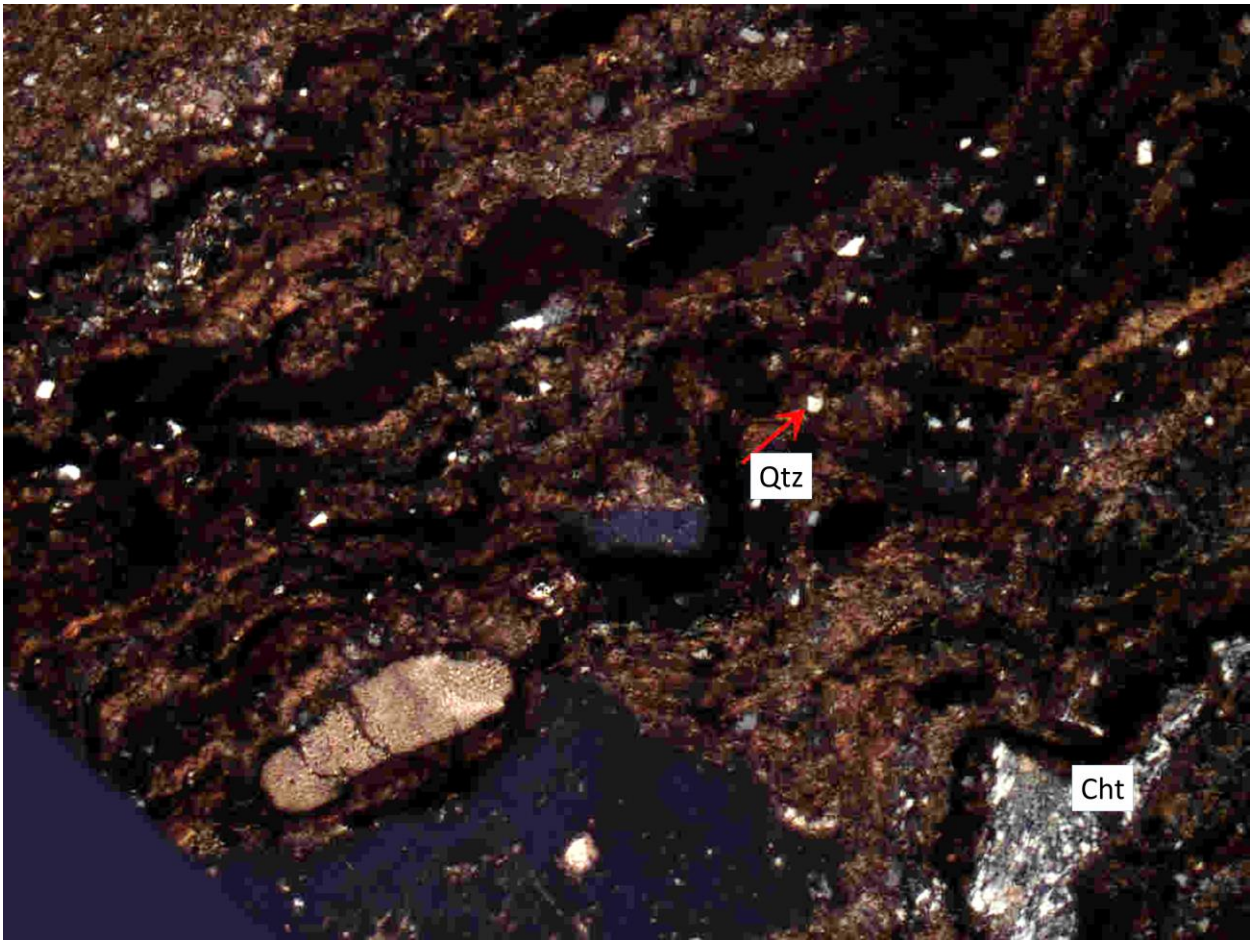


Figure 13. Photomicrograph of part of a shale clast from Flynn Creek breccia, which includes quartz grains (marked Qtz), chert grains (marked Cht), and a large fossil fragment (echinoderm). Provenance of this clast is most likely the lowermost Chattanooga Shale. Thin section 67-7-3-B; depth 21 m in drill core FC67-3. Cross-polarized light.

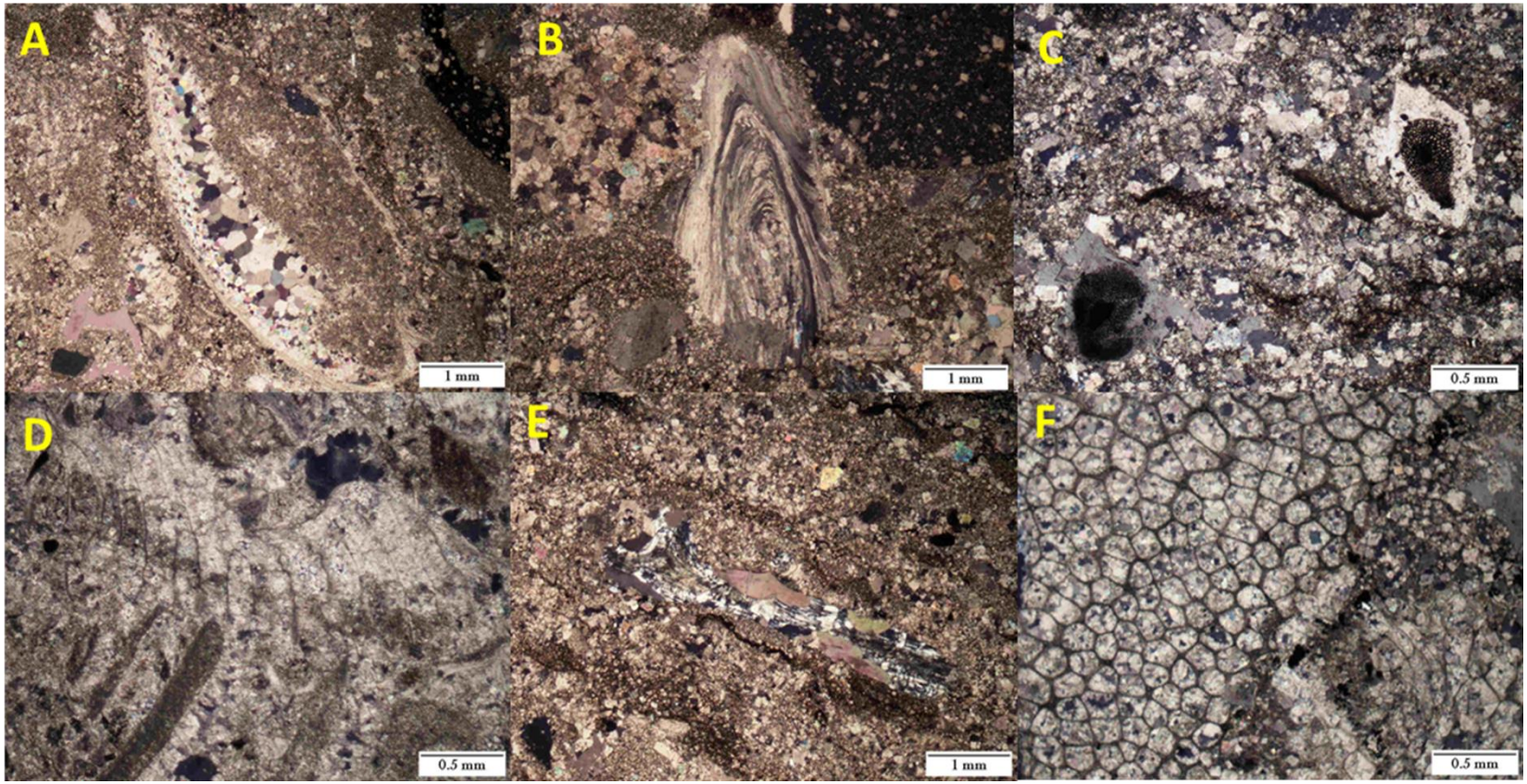


Figure 14. Representative photomicrographs of fossil fragments from Flynn Creek breccia. A and B: brachiopod (A shows geopetal structure); C: echinoderms (crinoids); D: coral-bryozoan grainstone clast; E: trilobite that is partially replaced by chalcedony; F: Coral. Cross-polarized light.

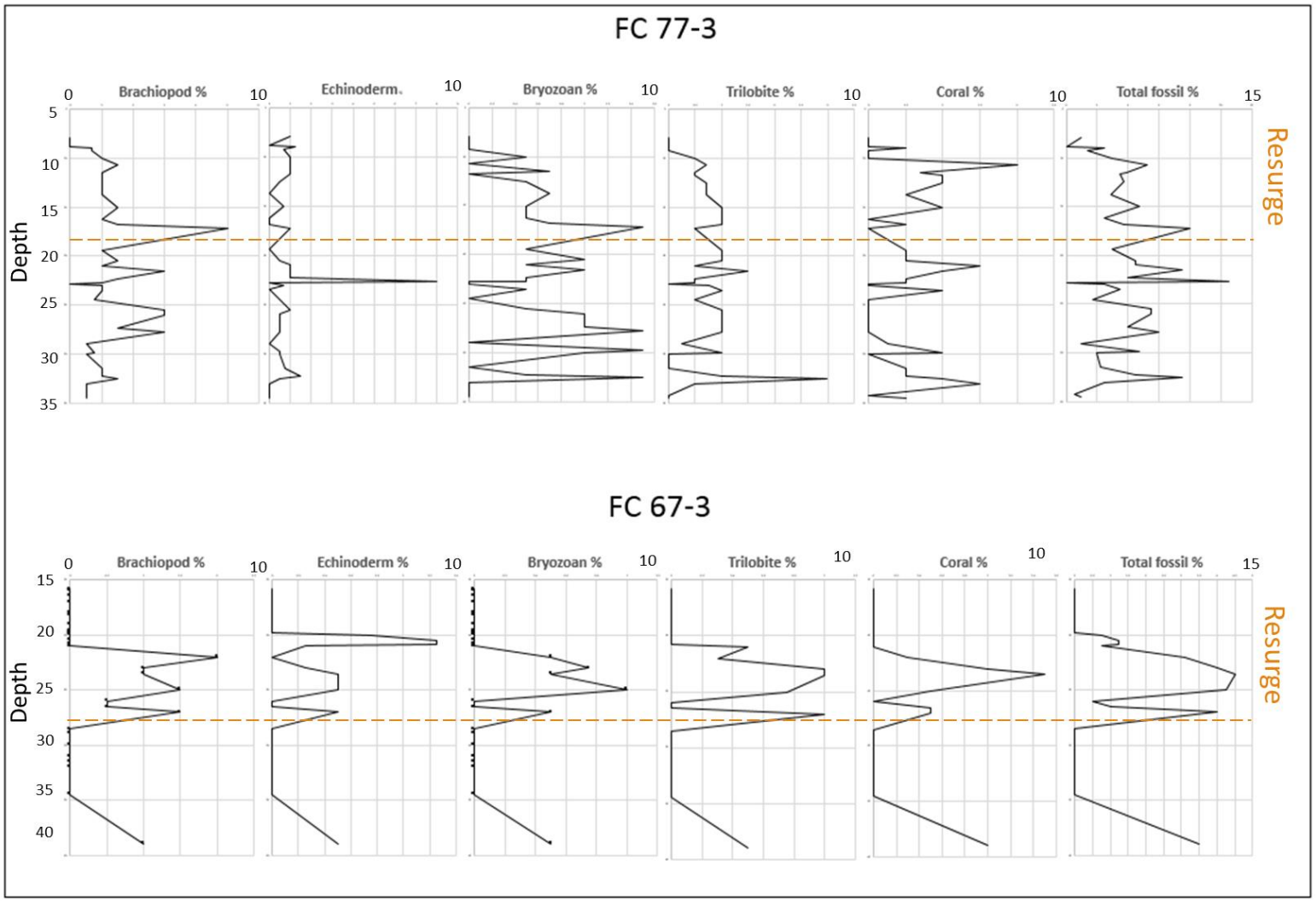


Figure 15. Vertical plots of volume percentage of fossils types and (at right) total fossil content for drill cores FC77-3 and FC67-3. Each dot represents the position of one thin section in that drill core. Depths in meters.

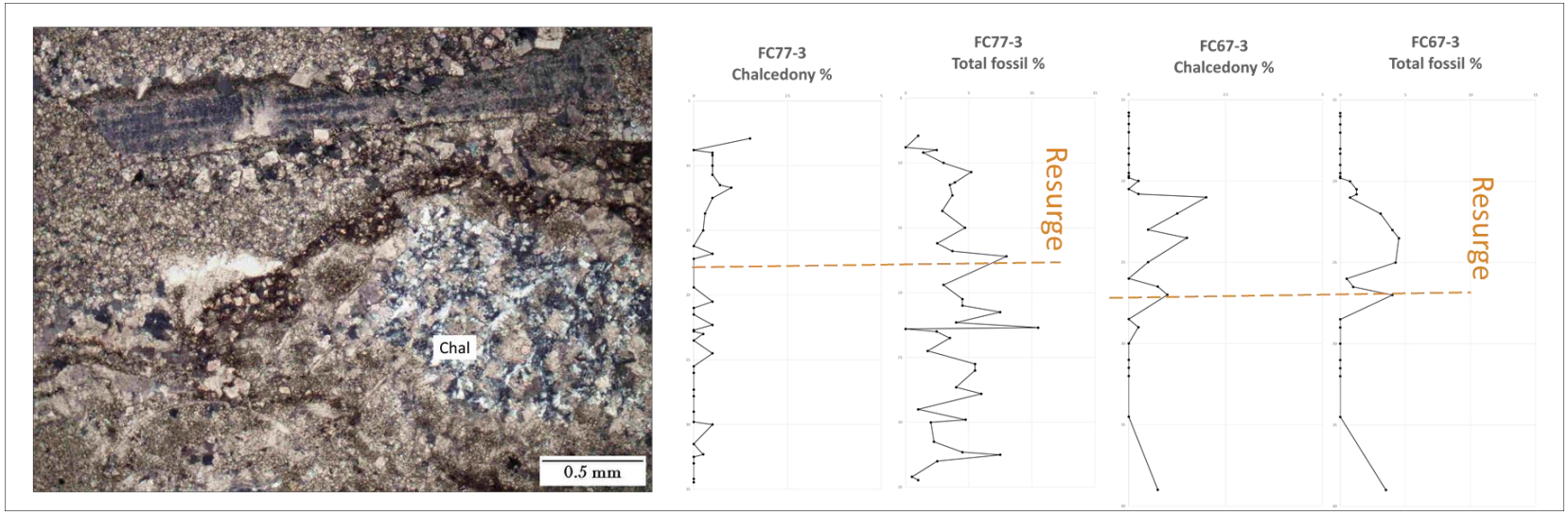


Figure 16. Representative photomicrograph of chalcedony (Chal) replacement of part of a coral fragment. Cross-polarized light. At right: Volume percentage with depth plots showing total fossil content in the Flynn Creek breccia as compared to the occurrence of chalcedony in both drill cores. The co-occurrence of fossil fragments, regardless of taxon, and chalcedony (both as discrete chalcedony grains and as fossil fragments with partial chalcedony replacement) is evident in both drill cores, but most obvious in FC67-3, between 28 and 20 meters depth. Each dot represents the position of one thin section in that drill core. Depths in meters.

In both drill cores examined, subangular to subrounded, silt-sized quartz grains occur dispersed within the fine-grained carbonate matrix (Fig. 17). In some instances, quartz grains also occur as rounded grains within rare shale clasts. Close to the breccia contact with the overlying Chattanooga Shale, quartz of a different type was observed. This is coarse sand- to granule-sized material, which is made up of quartz associated with carbonate grains, displaying concave-convex to sutured inter grain contacts. (Fig. 18).

Many of these rare clasts contain numerous, very small fluid inclusions and appear to be highly altered. Most quartz grains in the Flynn Creek breccia are equidimensional, however, some rare, highly elongated quartz grains occur in the upper part of the resurge breccia deposit near the transition point to very fine breccia (i.e., carbonate clast sizes under 5 mm). Quartz grains ranging in size from fine sand to granules occur in the basal bed of the Chattanooga Shale, and thus the quartz we see in the resurge may have been included within the proximal ejecta (and thus resurge deposits) derived from the same basal phosphatic sandstone or "blue phosphate" as noted above.

Figure 17 also shows the quartz volume percentage graphs of the present study and these data give an overview of the quartz-grain occurrence through both drill cores. Samples from drill core FC67-3 show oscillating values between 0 and 2% through most of the breccia deposit, but there are two small abundance peaks (4 and 6%) located between 19 and 20 m depth. This depth is within the aqueous resurge part of crater-filling unit. Samples from drill core FC77-3 also show most volume percentage values ranging from 0 to 2%, but there is a peak also at the bottom of the deposit (4%) and close to the contact with the overlying Chattanooga Shale (6%). This peak includes the coarse quartz clasts noted above.

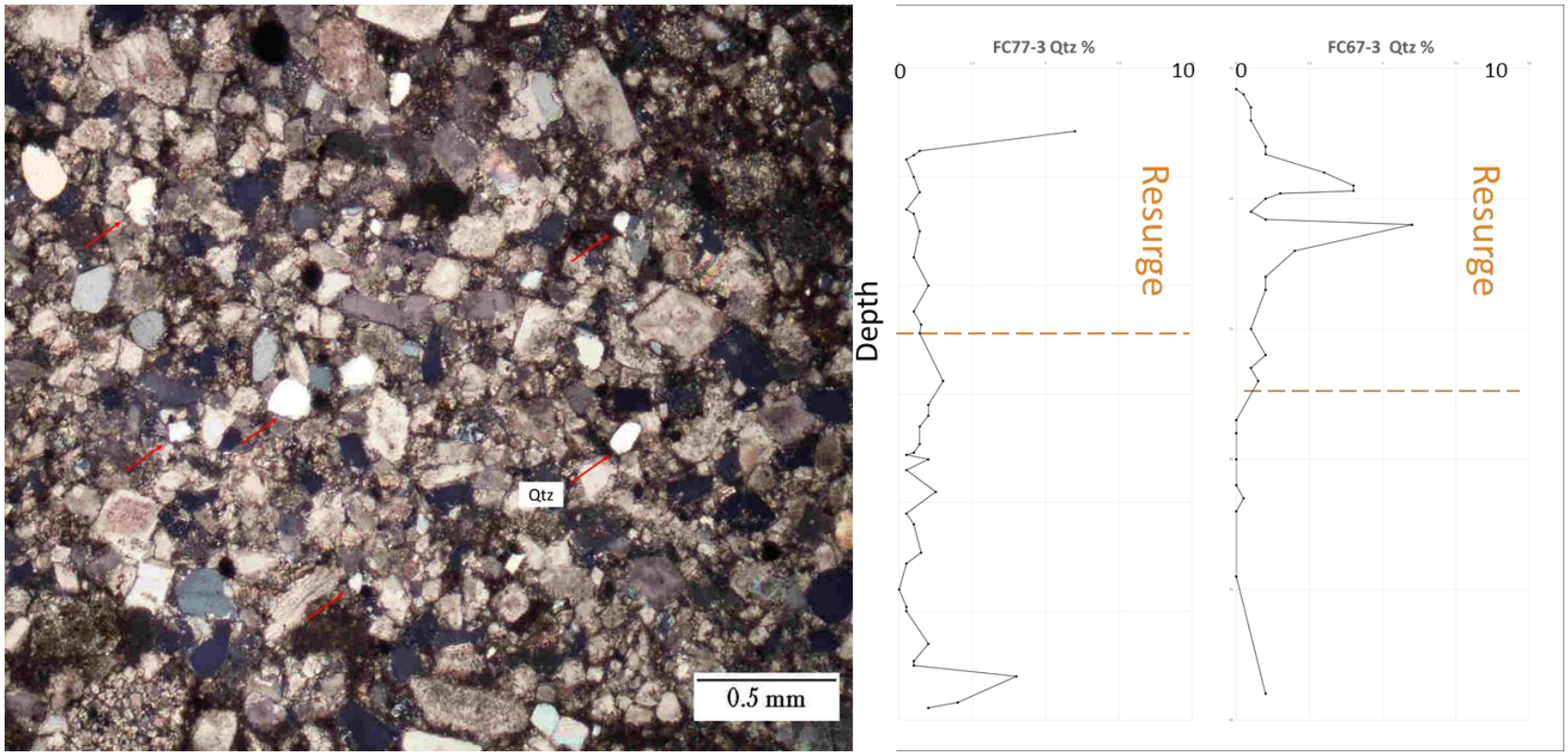


Figure 17. Representative photomicrograph of sub-rounded, fine-sand sized quartz grains (Qtz), which are dispersed within the Flynn Creek breccia's carbonate matrix. Cross-polarized light. At right: Volume percentage with depth plots showing total quartz grain occurrence in the Flynn Creek breccia in both drill cores. Each dot represents the position of one thin section in that drill core. Depths in meters.

Matrix in the Flynn Creek breccia is a mixture of micrite, finely macerated fossil material, fine pellets, fine carbonate clasts, and other very small but not identifiable crystalline materials. Matrix has been replaced in some instances by secondary dolomite and modified by compaction and post-impact stylolite development. Figure 19 shows the matrix volume percentage for both drill cores as examined petrographically. Both drill cores show relatively similar overall percentage curves. These similar curves show relatively low matrix content within the lower part of the resurge breccia deposit, which was characterized megascopically as

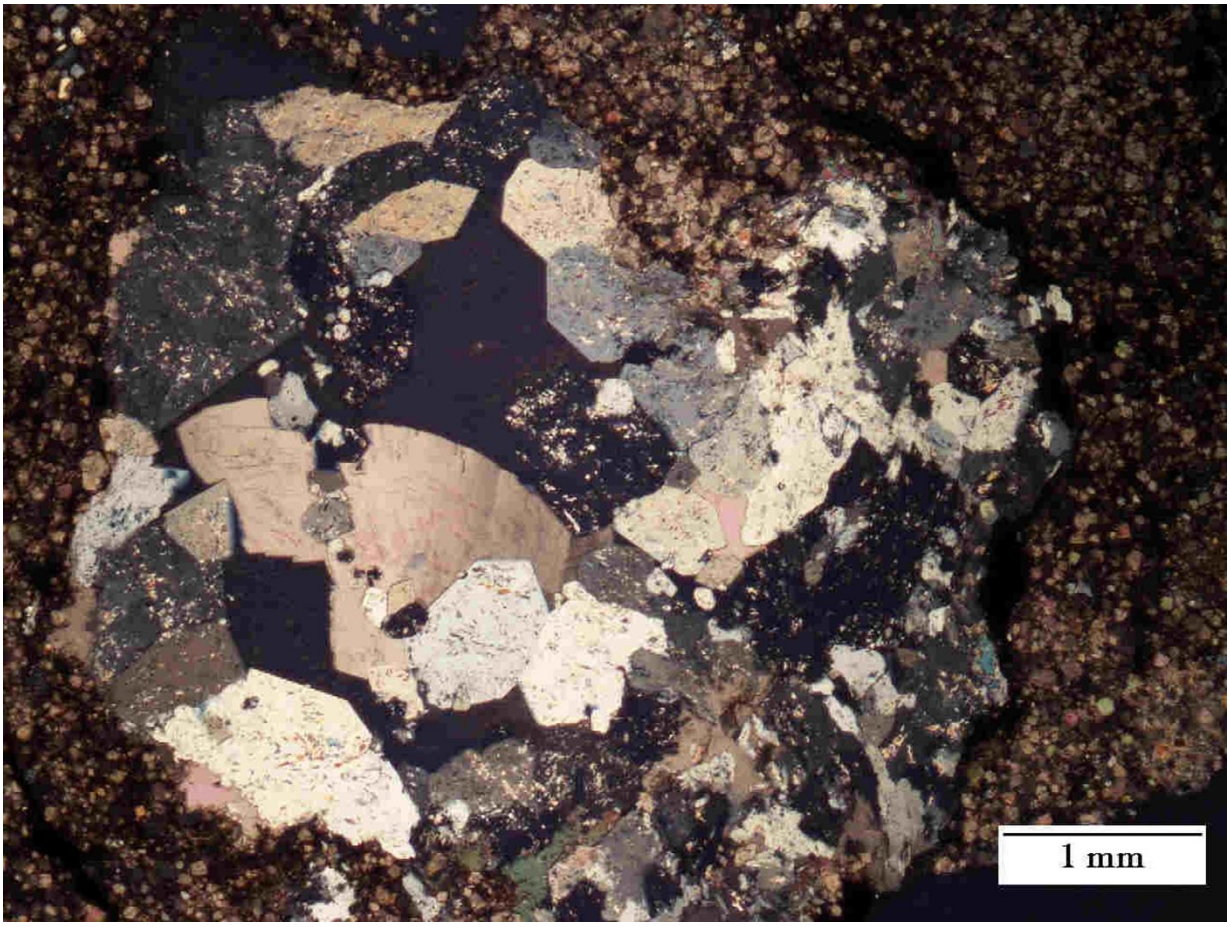


Figure 18. Photomicrograph of one of the quartz granules that composed of multiple quartz crystal domains with concave-convex to sutured inter-granular crystal contacts. Granule shows internal alteration effects that may be impact-related, including numerous fluid inclusions and undulose extinction. Thin section 77-3-5-A; depth 7.9 m in drill core FC77-3. Cross-polarized light.

having a clast-supported texture (De Marchi, et al. 2018, in review). Within the normally graded resurge deposit, as the grain size decreases, matrix percentage increases and becomes a substantial part of the deposit. Near and at the top, matrix makes up almost the totality of the upper very fine-grained sediments. At and near the bottom of the crater-fill breccia deposit, diagenetic features that were likely induced by physical compaction of crater-filling sediments occur. These features include stylolites and calcite-filled fractures (Fig. 20). The fact that they are concentrated at the bottom of the deposit also might be related to the larger clast size of blocks in that part of the breccia (i.e., up to 2.13 m in FC67-3 and up 3.40 m in FC77-3), wherein these features are more likely to be observed. Evenick et al. (2004) identified Flynn Creek stylolites as being melt features, but these features at Flynn Creek are no different from other stylolites in carbonate rocks world-wide, and there has been agreement for decades on their compaction-related origin by gradual and selective dissolution.

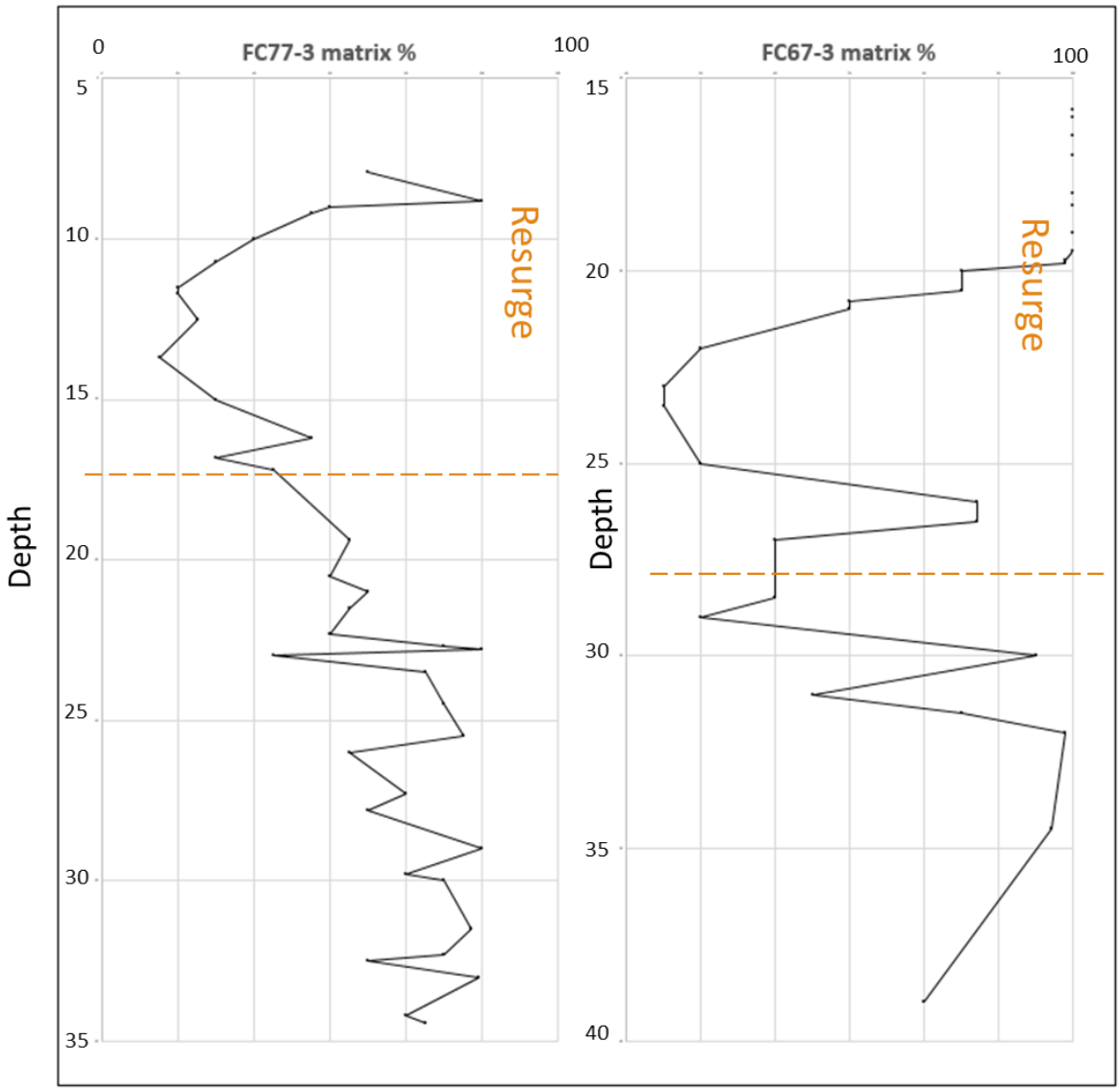


Figure 19. Vertical plots of volume percentage of matrix for drill cores FC77-3 and FC67-3. Each dot represents the position of one thin section in that drill core. Depths in meters.

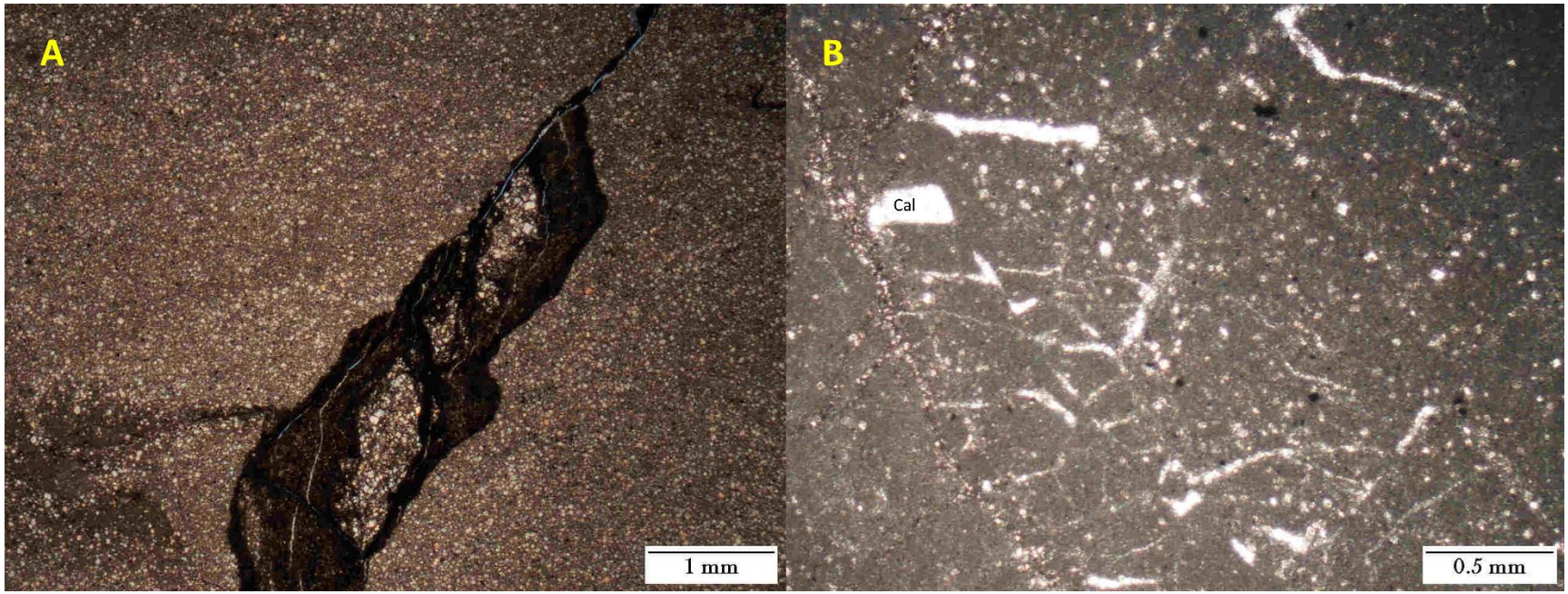

Figure 20. Representative photomicrographs of Flynn Creek breccia stylolite (A) and calcite filled fractures (B), which are relatively common features in some clasts within the lower part of the slump-emplaced deposit within the crater moat-filling deposit. A and B - thin section FC67-11-1-A in drill core FC67-3; depth 34.5 m. Cross-polarized light.

In the systematic petrographic search for impact-related features, such as melt particles and quartz deformation features (e.g., PFs (planar fractures) and PDFs (planar deformation features), numerous melt particles were found, but few impact-affected quartz grains. Regarding PFs and PDFs in quartz, one single occurrence of PFs was found and one set of possible PDFs was found as well among all the 70 thin sections examined. Both of these apparently impact-affected quartz grains were found within shale clasts (Fig.21). Even though these features look promising as shock-induced microstructures, the PDFs are far too few and not clearly developed enough to conclude they are definitive as impact features at this time. Finding these grains, however, may suggest that eventually a larger population of such grains may be found in the USGS drill-core collection. Our results in looking for impact-affected grains mirrors the petrographic results of Adrian et al. (2018) who looked at one central uplift drill core of 175 m length from Flynn Creek and found numerous melt clasts but no impact-affected quartz grains.

Two different types of melt clasts were identified, and both types occurred in both drill cores. Melt type 1 (grey silica melt), which has as reported once previously at Flynn Creek (Adrian et al., 2018), is a cryptocrystalline melt that is characterized by extremely finely crystalline quartz that appears isotropic (i.e., the isotropic phase appears dark with cross-polarized illumination, but there is a fine crystallinity nevertheless – see the discussion in Adrian et al., 2018). Melt type 1 commonly has euhedral dolomitic inclusions and may have anhedral inclusions of other materials as well. Size of melt type 1 ranges up to 15 mm in drill core FC77-3 and up to 2 mm in FC67-3. Particles of melt type 1, as described by Adrian et al. (2018), are much larger – up to 1 cm or more – but it should be noted that they come from the central uplift area of Flynn Creek, not the crater moat as described here. Similar-appearing silicate impact melt has been reported by Osinski et al. (2005) from within the crater-filling breccias of Haughton impact structure, a

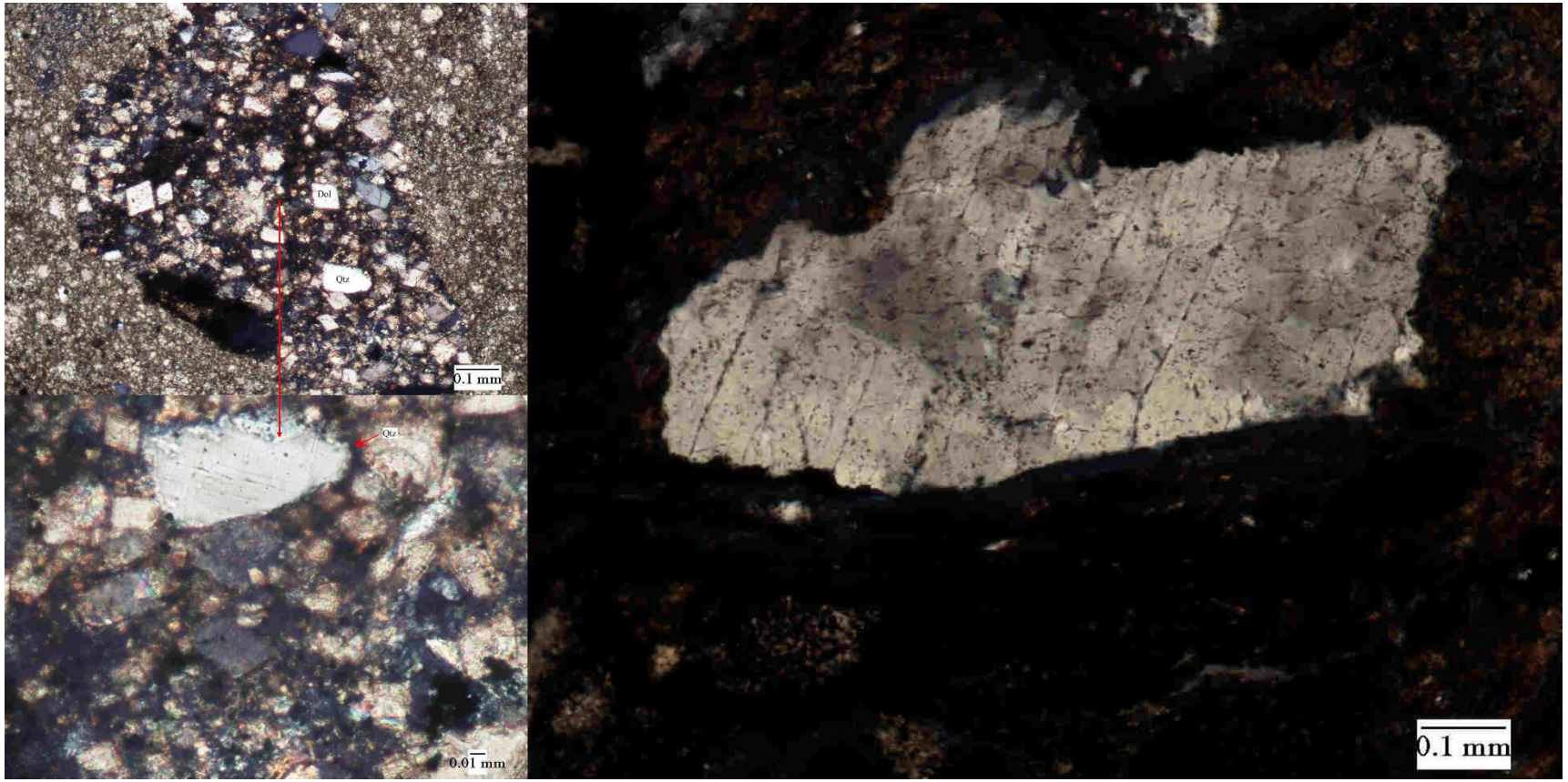


Figure 21. Possible planar deformational features (PDF) (lower left) in thin and planar fractures (PF) (right) in quartz grains within one dolomitized shale clast (upper left). Thin section FC67-7-3-B; depth 21 m in drill core FC67-3. Cross-polarized light.

carbonate-target impact on Devon Island, Canada. The silicate glasses described at Houghton contain substantial amounts of CaO and/or calcite occurring as globules or euhedral zoned crystals. These inclusions are related to calcite-cemented sandstone clasts presents within Houghton's impact breccia deposits (Osinski et al., 2005).

The shape of melt type 1 particles range from angular to rounded in drill core FC77-3 and from angular to sub-rounded in drill core FC67-3. At the bottom of FC77-3 this melt occurs as a dispersed mass with irregular boundaries.

Figure 22 shows plane light and cross-polarized light views of two different Flynn Creek silicate melt occurrences with and without inclusions along with their volume percentage estimations in each drill cores. The graph of volume percentage of melt in drill core FC67-3 shows these particles are more common at or near the bottom of the deposit, and also in between 20 and 30 m depth. Depths of 20 to 30 m comprise resurge and intermingled slumping deposits in FC67-3. In contrast, in drill core FC77-3, a relatively high concentration of melt is at the bottom (in fall back materials) and oscillating values for melt particles toward the top of the deposit indicate an increase upwards within the marine resurge part of the breccia deposit. In drill core FC67-3, the highest melt peak is located at 21 meters depth, which represents a thin section made from a sample with a rare shale clast that contains type 1 melt.

Both drill cores examined in this study show melt particles at or near their bases, and those occurrences can be related to first stage of crater filling (i.e., fall back of incandescent materials). Melt particles above the lower levels likely were entrained in the slumping and subsequent resurge events within the crater-moat area.

Qualitative microprobe analysis of a grey silica (type 1) melt particle containing dolomite crystals, located at 26 m depth on drill core FC67-3, were performed through BSE

images and stage scan mapping of Ca, Mg, Fe, and Si. Figure 23 displays images obtained showing high silica content in the melt fragment and, as expected, a Ca-Mg response for dolomitic inclusions and surrounding matrix. BSE and Fe mapping also shows iron-rich inclusions within the melt particles, and additional analysis in the center of this crystal, in EDS mode, revealed the presence of sulfur.

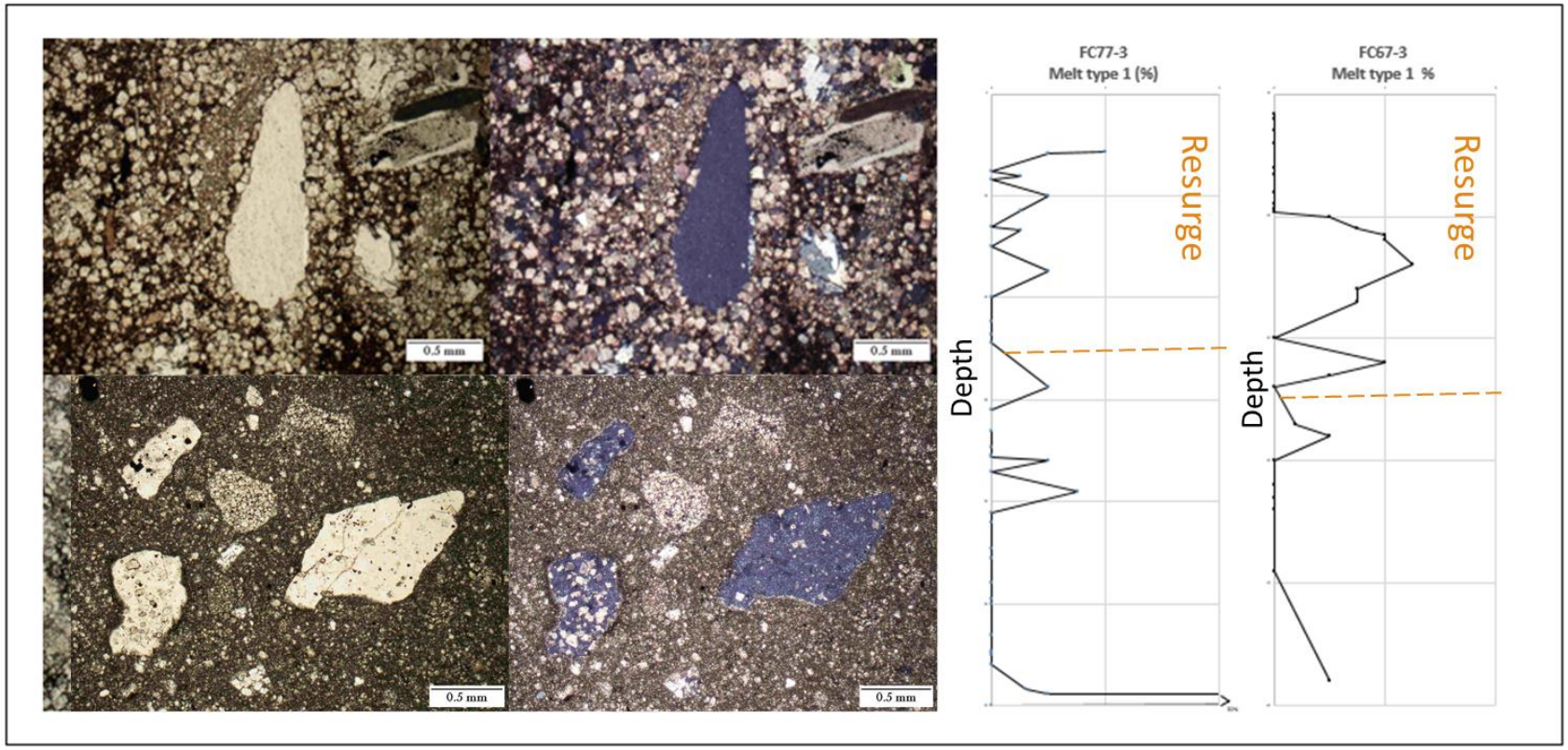


Figure 22. Photomicrograph grouping on the left – Plane light (left) and cross-polarized view (right) of type 1 (silica-rich) melt clasts, with and without dolomitic inclusions. At right – Volume percentage with depth plots showing type 1 (silica-rich) melt distribution through drill cores FC77-3 and FC67-3. Each dot represents the position of one thin section in that drill core. Depths in meters.

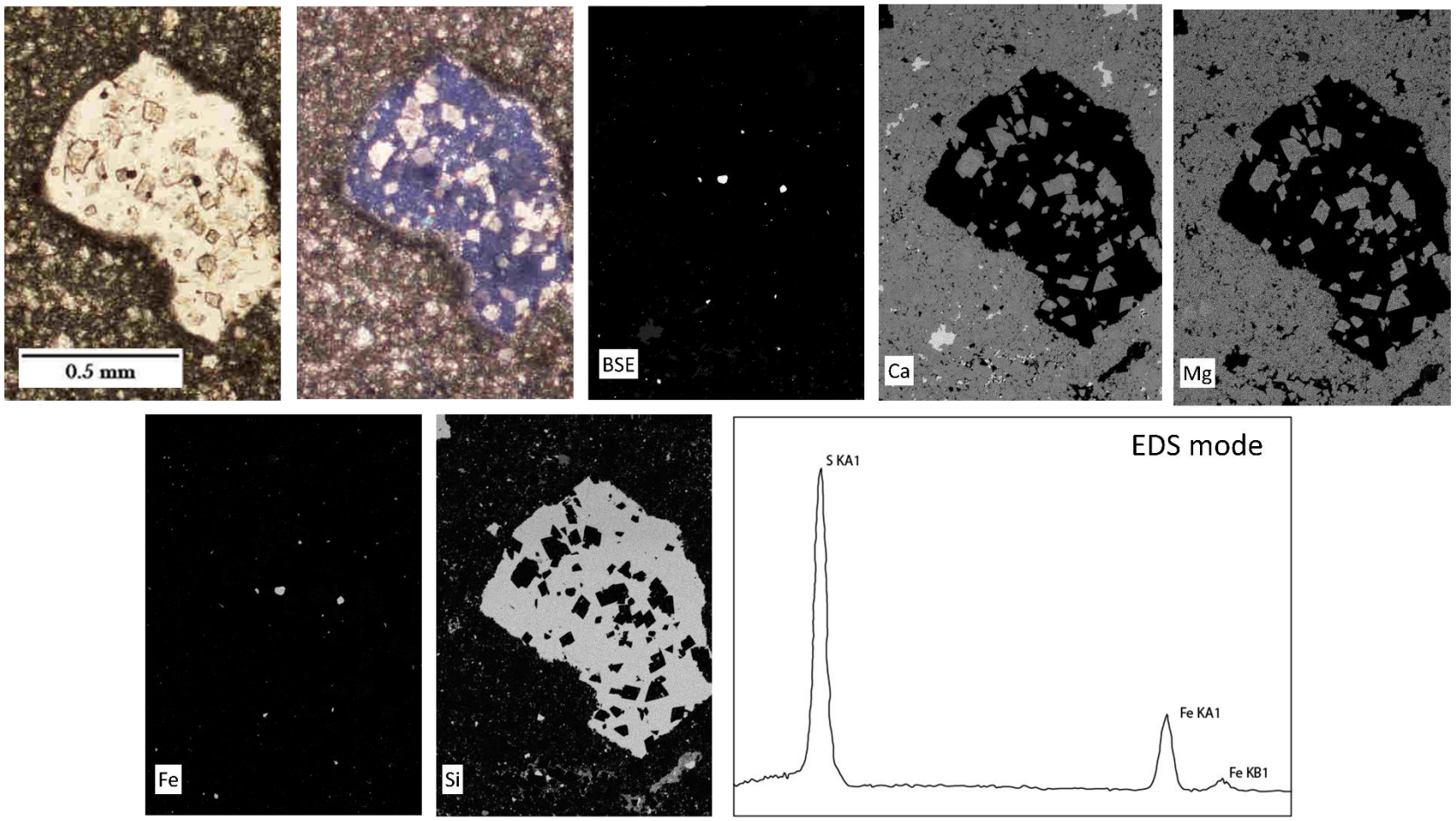


Figure 23. Type 1 (silica-rich) melt clasts. Upper row, first two images: Photomicrographs of example type 1 melt particle containing rhombic dolomite crystalss (left, plane light; right, cross-polarized light). Thin section FC67-8-1-A; depth 26 m in drill core FC67-3. Upper row: BSE micrograph and stage-scan mapping of same grain at same scale for Ca and Mg. Lower row: Stage-scan mapping of the same grain at same scale for Fe, and Si (as labeled on image), Lower right: EDS spectrum obtained with a beam focused on a high-Fe grain, showing peaks characteristic of pyrite.

Quantitative microprobe analysis was also performed on melt particle on thin section located near the bottom of crater fill deposit (Fig. 24). This analysis confirms high silica content in these melts, but also shows minor, but noteworthy, concentrations of Al and also traces of Na, Mg, K, Ca, Fe, and Mn. The presence of these different elements may indicate melting of multiple types of materials and/or meteoritic contributions.

Another type of melt particle is a new phase of melt that we refer to here as melt type 2. Type 2 melt was identified within both drill cores of the present study is characterized by a distinctive amber color when observed petrographically using transmitted light. This melt type, like type 1, appears to be isotropic, judging from the lack of transmission of cross-polarized light (Figs. 25-27), but its finer particle size versus type 1 melt makes it difficult to assess any crystallinity at a nanoscale. This type of melt is superficially similar in appearance to phosphate-enriched fossil fragments in that they are both about the same color in transmitted light and they remain dark in cross-polarized light regardless of stage orientation. However, these melt grains display internal evidence of melting processes such as flow textures, micro-crystallite bundled inclusions, and inclusions of differently appearing materials, including opaque constituents (Fig. 27). Thus, they are clearly not fossil fragments, which show either no internal structure or organic laminations. The melt particles range from angular to rounded occurrences in both drill cores. On the bottom of FC77-3, these amber-colored particles occur with more irregular boundaries and flow textures.

Electron-microprobe analysis of a thin section containing these type 2 melt particles, which is located near the bottom of drill core FC77-67, was performed through BSE images and stage-scan mapping of Ca, Mg, and Si. This analysis showed a higher concentration of Ca

within these amber-colored glasses. Figures 26 and 27 display images obtained during these analyses.

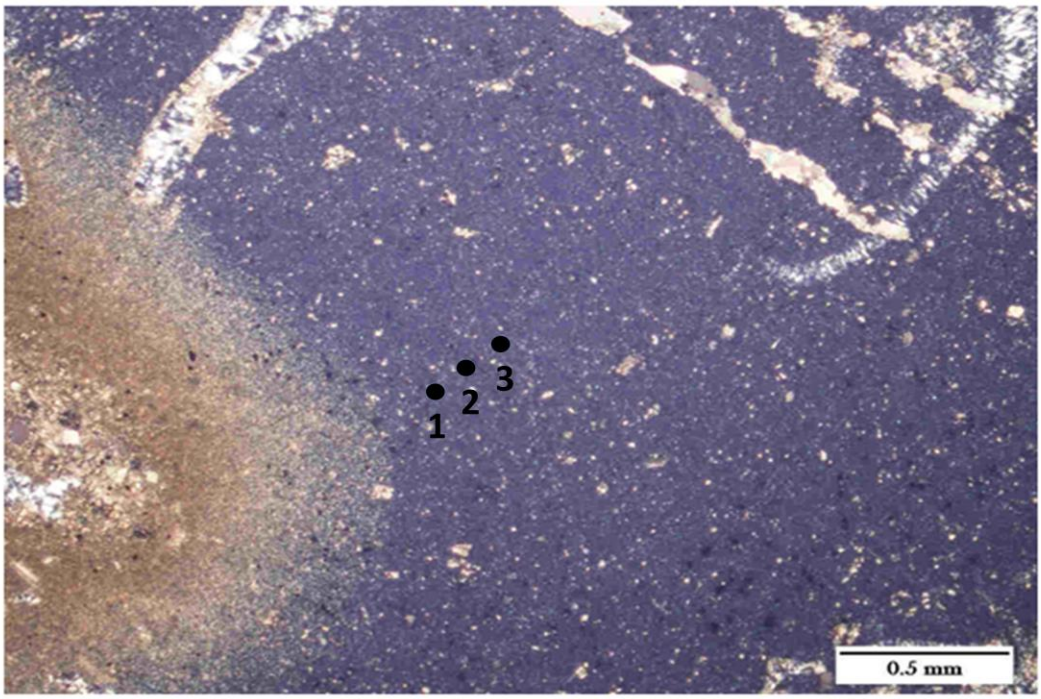


| Element | #1 | #2 | #3 |
|---|---|---|---|
| Na | 0.00 | 0.00 | 0.02 |
| Mg | 0.02 | 0.01 | 0.00 |
| Al2O3 | 0.14 | 0.34 | 0.28 |
| SiO2 | 99.81 | 98.85 | 99.56 |
| K | 0.00 | 0.03 | 0.05 |
| CaO | 0.00 | 0.00 | 0.02 |
| Fe | 0.00 | 0.00 | 0.00 |
| Mn | 0.04 | 00.00 | 0.000 |
| **Total** | **100.01** | **99.23** | **99.93** |

Figure 24. Photomicrograph (left) of interior of type 1 (silica-rich) melt clast with analytical spots marked. Right: Tabular results of quantitative analysis on melt clast for the three spots indicated. Thin section FC77-12-5-B from base of crater moat-filling breccia deposit in drill core FC77-3.

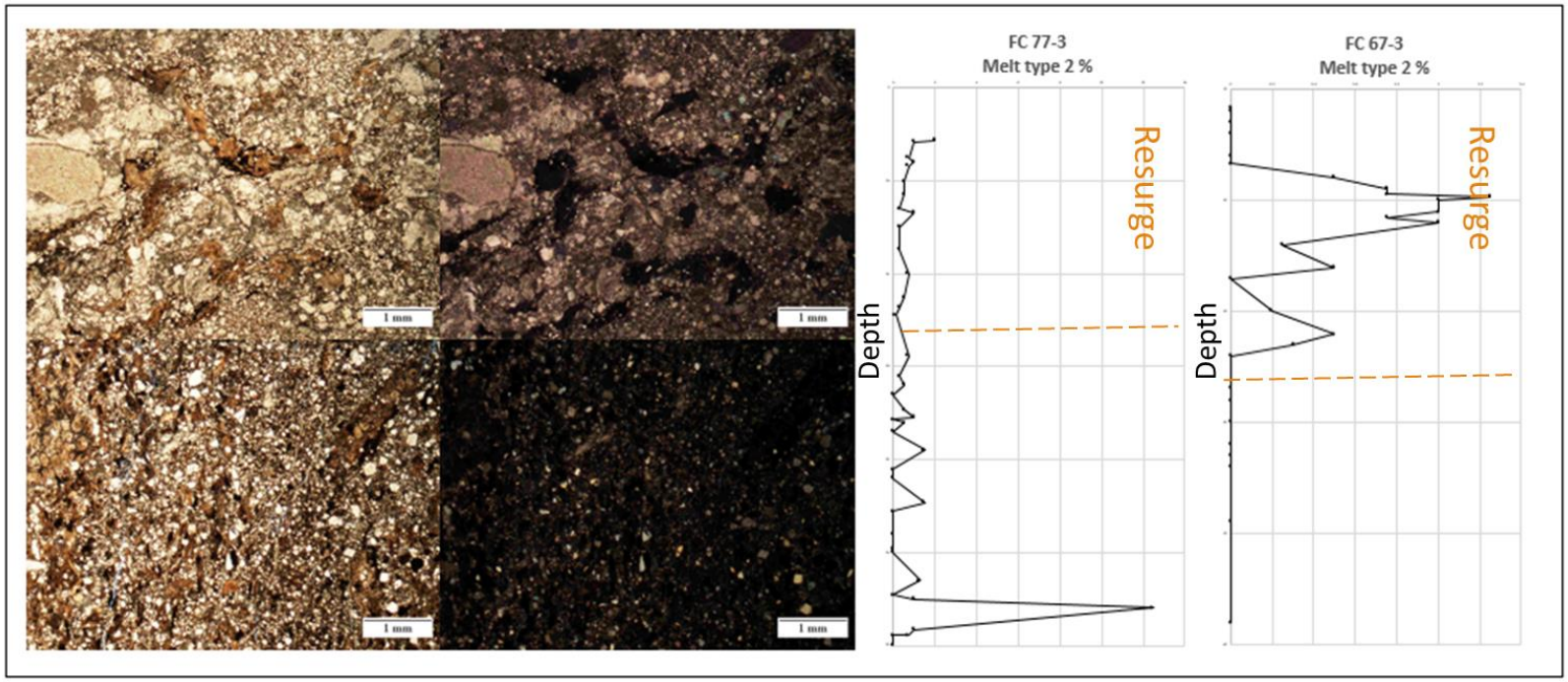


Figure 25. Photomicrograph grouping on left – Plane light (left) and cross-polarized view (right) of type 2 (phosphate-rich) melt particles (amber-colored). At bottom – Volume percentage with depth plots showing type 2 (phosphate-rich) melt distribution through drill cores FC77-3 and FC67-3. Each dot represents the position of one thin section in that drill core. Depths in meters.

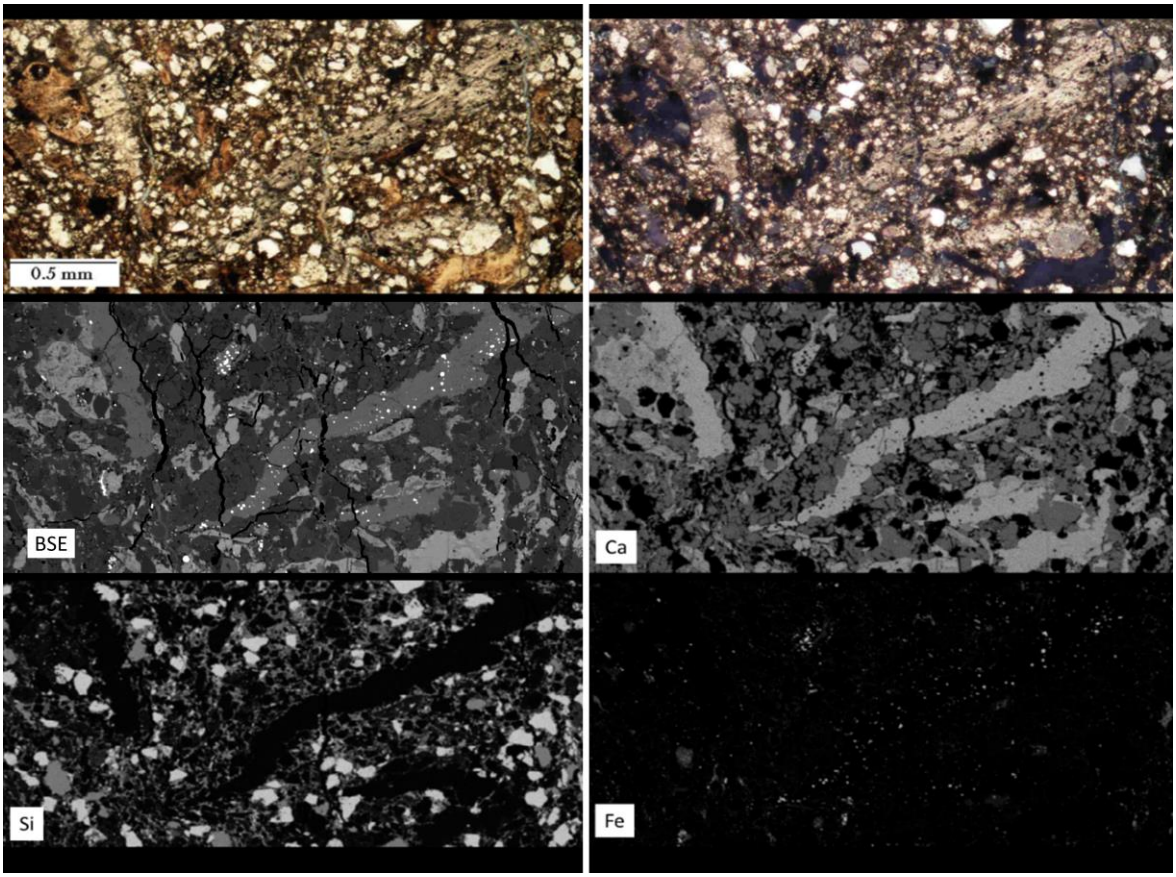


Figure 26. Type 2 (phosphate-rich) amber-colored melt clasts. Upper row, first two images: Photomicrographs of example type 2 melt particle (left, plane light; right, cross-polarized light). Thin section FC77-11-3-A; depth 33 m in drill core FC77-3. Middle row: BSE micrograph (left) and Ca stage-scan map of same thin-section area at same scale. Lower row: Stage-scan map of same area for Si and Fe (as labeled on image).

Complementary EDS analysis within a selected clast (see Fig. 27) indicates the presence of P, and suggesting a possible provenience of the melt as a phosphate-rich zone in the target materials. The Chattanooga Shale has just such a zone, which is a distinctive sandstone layer at the base of that formation, where it lies upon the eroded surface of local Upper Ordovician

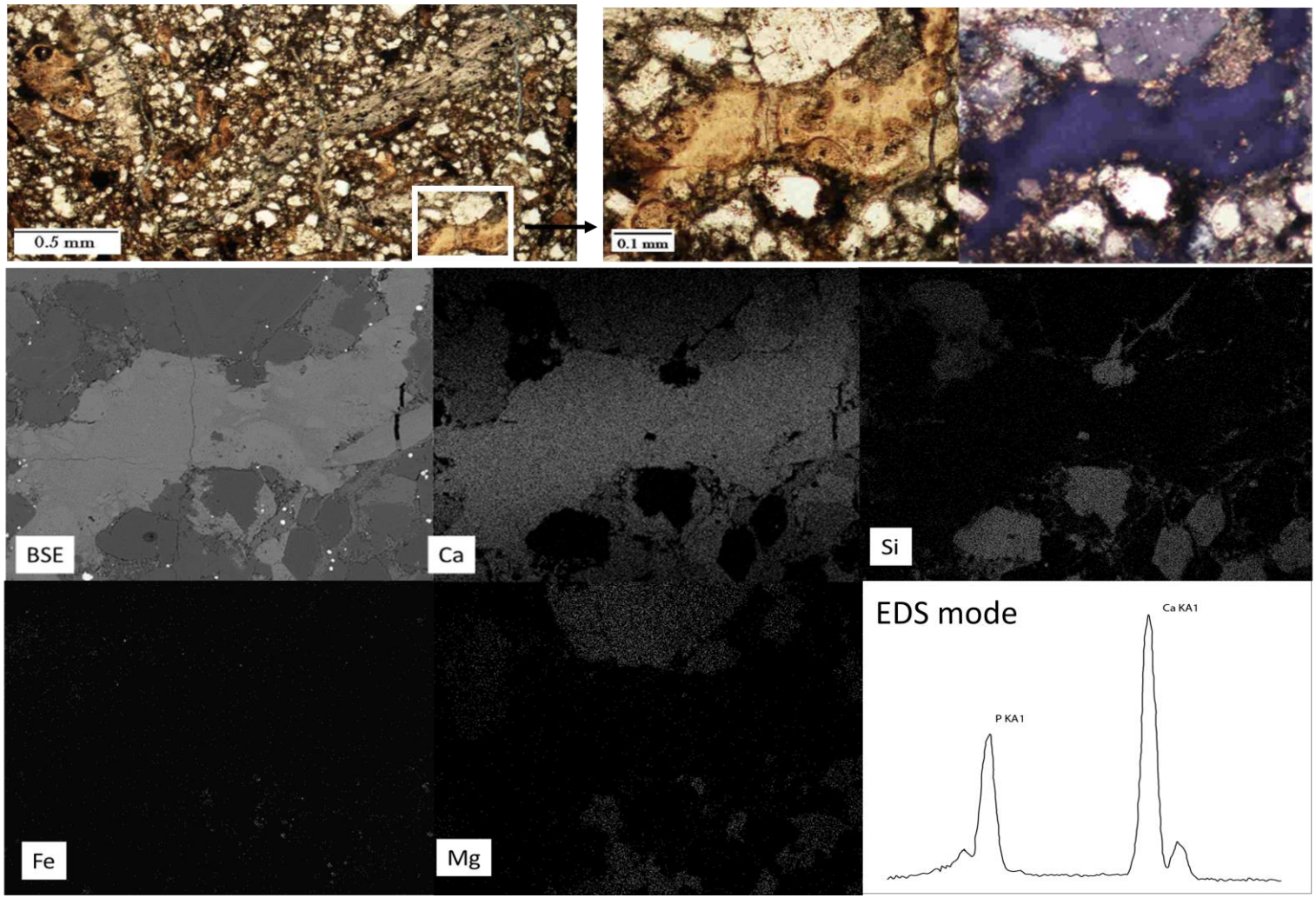


Figure 27. Type 2 (phosphate-rich) amber-colored melt clasts. Upper row, first two images: Photomicrograph of example type 2 melt particle (plane light) and enlargement of area (white box) with type 2 melt grain (plane light and cross-polarized) showing detail of internal melt-related structures (see text). Thin section FC77-11-3-A; depth 33 m in drill core FC77-3. Middle row: BSE micrograph of same enlarged area, Ca and Si stage-scan map of same area at same scale. Lower row: Stage-scan map of same area for Fe and Mg (as labeled on image) for same enlarged area, and EDS spectrum displaying peaks of P and Ca.

stratigraphy. Smith and Whitlatch (1940) were the first to study this fossiliferous, chalcedony-bearing, and phosphate-rich bed (regarding its potential to mine as an economic resource); and Conant and Swanson (1961) later remarked also on the peculiar nature of its mineralogy and basal setting (between Chattanooga and the underlying Catheys-Leipers Formation). That this bed could be, and likely is, the source of the phosphate-rich, amber-colored melt particles noted above is supported by the co-occurrence of these melt particles and pieces of chalcedony and chalcedony-replaced fossils, both of which are common clasts within the Chattanooga's distinctive basal sandstone, as are quartz sand grains and granules, according to references cited above. Comparison of the type 2 (phosphate-rich) melt particle distribution in the drill cores (Fig. 25) with the vertical distribution of total fossils (Fig. 15) and chalcedony (Fig. 16) shows this co-occurrence, especially with regard to drill core FC67-3.

## DISCUSSION

The timing of impact in relation to the local stratigraphic section has been a topic of research and discussion since the initial work of Roddy (1966; 1968). Roddy thought that at least some Chattanooga Shale would have to be in place so that rare shale clasts could be accounted for in what he called the bedded breccia. In looking at the Flynn Creek breccia in detail particularly regarding its age-diagnostic conodonts, Scheiber and Over (2005) concluded that there was a small population of basal Chattanooga conodonts admixed in the Flynn Creek breccia and that accounts for the breccia's currently accepted age of ~ 382 m.y. In recent drill-core studies of the genesis of the Flynn Creek impact-structure filling breccias, by both Adrian et al. (2018) and De Marchi et al. (2018; in review) concluded that only the lowermost section of Chattanooga Shale must have been in place at the time of impact because their detailed census of

thousands of breccia clasts revealed only a small handful of shale clasts. Now that our research of older stratigraphic literature (cited above) has shown that there is a basal bed of Chattanooga possessing the requisite mineralogy to explain the ejecta components found within the resurge of this same mineralogy, we suggest this is further evidence of impact during the very early, transgressive phase of deposition of the Chattanooga sea.

Previous work by Roddy (1968; 1979) established that Flynn Creek impact structure has a crater floor that is rather shallow as compared to many other craters, and upon which crater-filling deposits accumulated shortly after impact. Wilson and Roddy (1990) and Evenick (2005) noted that the crater-filling deposits were of two main types: non-bedded and bedded. Recent work by De Marchi et al. (2018; in review), which used core-analysis techniques such as line-logging and statistical analysis of line-logging data, has established that the non-bedded and bedded crater-filling deposits could be analyzed as to mode of emplacement. Specifically, the non-bedded or more chaotic breccias were fall-back and early slump deposits, and that marine resurge deposition and coeval slumping produced bedded breccias that are normally graded. These graded beds comprise the upper ~ 10-12 m of the crater-filling unit.

The analysis of drill cores FC67-3 and FC77-3 gives us a view of coeval crater-filling processes in opposite sides of the crater moat during early modification stage of this marine-target crater. In assessing asymmetry of crater-filling deposits, it is useful to look at each type of constituent in different points in the crater moat, as we have done here. Knowledge of the original placement for each rock type is quite useful to understand any crater. At Flynn Creek, however, the lithic and paleontologic similarity of the carbonate target units present in the area makes it exceedingly difficult if not impossible to determine the original source of each lithic and fossil clast. However, as noted above, reviewing the distribution of lithic and fossil clasts,

we have found a zone at the Chattanooga-Catheys-Leipers contact that is likely the source of many fossils, especially those with chalcedony replacement effects, chalcedonic masses, and phosphate clasts. In addition, quartz and feldspar sand and granules occur in this basal bed in the target area (Conant and Swanson, 1961), and these are included in the Flynn Creek ejecta and subsequent resurge deposits as well.

If we are correct about the source bed for fossils with chalcedony, chalcedonic masses, and phosphatic clasts, the ejecta components related to this suite should be symmetrically disposed around the crater and thus similarly disposed in the subsequent resurge deposits. However, the distribution of fossil fragments is not the same in the crater-moat filling breccias of the two drill cores examined in this study. In addition, the distribution of melt particles is not the same in the two drill cores examined. Without trying to interpret too much from our petrographic data, we tentatively advance the idea that ejecta asymmetry may have played a part in this uneven distribution of components within the two drill cores.

## CONCLUSIONS

The present study of the crater-filling breccias at Flynn Creek impact structure has shown that the filling sequence consisting of chaotic fall-back, mixed slump, and graded resurge deposits has petrographic characteristics that reveal more details about the breccia's possible disparate origins. In particular, there are two kinds of melt at Flynn Creek, a previously known "grey melt" (type 1) and a newly found, phosphate-rich amber-colored melt (type 2). Whereas the grey melt could have come from several possible sources in the impact target, including dispersed silica within the dolostones, the amber-colored melt must originate from a phosphate-rich zone. There is such a zone, the basal bed of the Chattanooga Shale, which also happens to

be rich in fossils, fossils with chalcedony, phosphatic fossil grains and clasts, and quartz sand and granules. This mineralogical suite occurs in the aqueous resurge section of the crater fill, which is interpreted to be largely ejecta washed back into the crater by the return flow of seawater. Asymmetry of the abundances of these distinctive components suggests possible asymmetry of ejecta during impact.

## ACKNOWLEDGEMENTS

The authors thank the National Aeronautics and Space Administration, Planetary Geology and Geophysics Program, for supporting the project proposal by J. J. Hagerty and others (NASA PGG NNH14AY73I) from which we derived support for this work. And we thank the staff of the USGS Flagstaff, particularly Tenielle Gaither and her associates, for help in providing cut drill-core samples to us. Also, we thank The Barringer Family Fund for Meteorite Impact Research for their support and the Astrogeology Branch of the U.S. Geological Survey in Flagstaff, Arizona, for organizing the Flynn Creek drill-core collection, hosting our visit to work on these materials, and providing many forms of assistance in sampling. The work by Ormö has been partially supported by grants AYA2008-03467/ESP, AYA2011-24780/ESP, AYA2012-39362-C02-01, ESP2014-59789-P, and ESP2015-65712-C5-1-R from the Spanish Ministry of Economy and Competitiveness and Fondo Europeo de Desarrollo Regional.

## REFERENCES

Adrian, D. R., King Jr, D. T., Jaret, S. T., Ormö, J., Petruny, L.W., Hagerty, J. J., and Gaither, T.

A. 2018. Sedimentological and petrographic analysis of drill core FC77-1 from the flank of the central uplift, Flynn Creek impact structure, Tennessee. *Meteoritics & Planetary Science*, v. 53, p. 857-873.

Adrian, D. R., D. T. King, Jr., and J. Ormö, in review, Resurge gullies and the 'inverted sombrero',Flynn Creek impact structure, Tennessee: *Meteoritics & Planetary Science*.

Conant, L.C. and Swanson, V. E. 1961. Chattanooga Shale and related rocks of central Tennessee and nearby areas. U. S. Geological Survey Professional Paper 357, 88p.

De Marchi, L., J. Ormö, D.T. King, Jr., and D.R. Adrian, 2018, Marine resurge sequences and interpreted processes at Flynn Creek impact structure, Tennessee: Lunar and Planetary Science [Lunar and Planetary Science Conference abstracts], v. 49, abstract no. 2323.

De Marchi, L., J. Ormö, D. T. King, Jr., D. R. Adrian, J. J. Hagerty, and T. A. Gaither, in review, Evidence of marine resurge sequences at Flynn Creek impact structure, Tennessee: *Meteoritics & Planetary Science*.

Dunham, R. J. 1962, Classification of carbonate rocks according to depositional texture. In: Ham, W. E. (ed.), *Classification of carbonate rocks*: American Association of Petroleum Geologists Memoir, p. 108-121.

Evenick, J.C., 2005, Field Guide to the Flynn Creek Impact Structure: Knoxville, University of Tennessee, 22 p.

Evenick J. C., Lee P., and Deane B. 2004. Flynn Creek impact structure: New insights from breccias, melt features, shatter cones, and remote sensing (abstract #1131). 35th Lunar and Planetary Science Conference. CD-ROM.

Evenick, J. C., and Hatcher, R. D., Jr. 2007. Geologic map and cross sections of the Flynn Creek

impact structure, Tennessee. GSA Map and Chart Series 95. Boulder, Colorado. Geological Society of America. 1:12,000.

King, D.T., Jr., Petruny, L.W., De Marchi, L., Chinchalkar, N.S., and Adams, M.C., 2018. sub Crater breccias, Flynn Creek impact structure, Tennessee: (abstract #2494). 49th Lunar and Planetary Science Conference. CD-ROM.

Osinski, G.R., Spray, J.G., and Lee, P. 2005. Impactites of the Haughton impact structure, Devon Island, Canada High Artic: *Meteoritics & Planetary Science*, v. 40, p. 1789-1812.

Roddy, D. J. 1966. The Paleozoic crater at Flynn Creek, Tennessee [dissertation]. Pasadena, California. California Institute of Technology. 232p.

Roddy, D. J. 1968. The Flynn Creek crater, Tennessee. Edited by French, B. M., and Short, N. M. *Shock and Metamorphism of Natural Materials*. Baltimore, Maryland. Mono Book Corporation. pp. 291–322.

Roddy, D. J. 1979. Structural deformation at the Flynn Creek impact crater, Tennessee: a preliminary report on deep drilling. *Lunar and Planetary Science* 10:2519-2534.

Roddy D. J. 1990. Structure Contour Map Drawn on the Base of the Chattanooga Shale Flynn Creek Crater, Gainesboro Quadrangle, Tennessee. Edited by Hill W. T., Tennessee Division of Geology, Scale 1:12,000.

Scheiber, J. and Over, J. D. 2005. Sedimentary fill of the Late Devonian Flynn Creek crater: a hard target marine impact. Edited by Over, D. J., Morrow, J. R., and Wignall, P. B. *Understanding Late Devonian and Permian-Triassic Biotic and Climatic Events: Towards and Integrated Approach*. New York. Elsevier. pp. 51-69.

Smith, R. W. and Whitlatch, G. I. 1940. The phosphate resources of Tennessee. *Tennessee Department of Conservation, Division of Geology, Bull*. 48, 1.

Terry, R. D. and Chilingar, C. V. 1955. Comparison charts for visual estimation of percentage composition. *Journal of Sedimentary Petrology,* vol. 25, n. 3, p. 229-234.

U. S. Geological Survey, 2017. Mineral Resources On-Line Spatial Data. http://mrdata.usgs.gov

Wilson, C. W., Jr. and Roddy, D. J., 1990. Geologic map and mineral resources summary of the Gainesboro quadrangle, Tennessee: Tennessee Division of Geology, GM 325-SW, Scale 1:24,000.

# Conclusions

Flynn Creek crater-moat deposits are characterized by ~30-m thick breccia sequence which is divided by four different types of depositional processes: Fall-back, slumping from the rims, slumping caused by central peak collapse, and normally graded resurge deposits. Evidence presented here and in previous work indicates that, at the time of the impact, the target Upper Ordovician bedrock carbonates were just beginning to be overlain by thin, basal beds of the transgressive Upper Devonian Chattanooga Shale, which is the main unit that overlies the entire structure. Granulometric and statistical analysis of crater-filling breccias in two drill cores studied herein show many important similarities with other Paleozoic marine target impact structures, Lockne (~ 7.5 km) and Tvären (~ 2 km), and the larger Eocene marine impact structure, Chesapeake Bay (~ 40/85 km). Petrographic characteristics reveal two kinds of melts at Flynn Creek, a previously known "grey melt", which could have come from silica rich regions within the target, and a newly found, phosphate-rich "amber melt", which is likely derived from the basal bed of the Chattanooga Shale, which contains phosphatic fossil grains and clasts. Variations regarding deposit content, such as melt particles, fossils, and quartz grains, between two different sides of the crater indicates an asymmetry, which is possibly related to an un-even distribution of the ejecta material during impact.

Combined References

Adrian, D.R., King Jr, D. T., Jaret, S. T., Ormö, J., Petruny, L.W., Hagerty, J. J., and Gaither, T. A. 2018. Sedimentological and petrographic analysis of drill core FC77-1 from the flank of the central uplift, Flynn Creek impact structure, Tennessee. *Meteoritics & Planetary Science*, v. 53, p. 857-873.

Adrian, D. R., D. T. King, Jr., and J. Ormö, in review, Resurge gullies and the 'inverted sombrero', Flynn Creek impact structure, Tennessee: *Meteoritics & Planetary Science*.

Azad, A. S., Dypvik, H., and Kalleson, E. 2015. Sedimentation in marine impact craters – Insight from the Ritland impact structure. *Sedimentary Geology* 318:97-112.

Conant, L. C. and Swanson, V. E. 1961. Chattanooga Shale and related rocks of central Tennessee and nearby areas. U. S. Geological Survey Professional Paper 357, 88p.

Costa, J.E., 1988. Rheologic, geomorphic, and sedimentologic differentiation of water floods, hyperconcentrated flows, and debris flows, *in* Baker, V.R., Kochel, R.C., and Patten, P.C. (eds) Flood Geomorphology: Wiley-Intersciences, New York, p. 113-122

De Marchi, L., J. Ormö, D.T. King, Jr., and D.R. Adrian, 2018, Marine resurge sequences and interpreted processes at Flynn Creek impact structure, Tennessee: Lunar and Planetary Science [Lunar and Planetary Science Conference abstracts], v. 49, abstract no. 2323.

De Marchi, L., J. Ormö, D. T. King, Jr., D. R. Adrian, J. J. Hagerty, and T. A. Gaither, in review, Evidence of marine resurge sequences at Flynn Creek impact structure, Tennessee: *Meteoritics & Planetary Science*.

Dunham, R. J. 1962. Classification of carbonate rocks according to depositional texture. In: Ham, W. E. (ed.), *Classification of carbonate rocks*: American Association of Petroleum Geologists Memoir, p. 108-121.

Evenick, J.C., 2005. Field Guide to the Flynn Creek Impact Structure: Knoxville, University of Tennessee, 22 p.

Evenick J. C., Lee P., and Deane B. 2004. Flynn Creek impact structure: New insights from breccias, melt features, shatter cones, and remote sensing (abstract #1131). 35th Lunar and Planetary Science Conference. CD-ROM.

Evenick, J. C., and Hatcher, R. D., Jr. 2007. Geologic map and cross sections of the Flynn Creek impact structure, Tennessee. GSA Map and Chart Series 95. Boulder, Colorado. Geological Society of America. 1:12,000.

Folk, R. L. 1974. *The petrology of sedimentary rocks*. Austin, Texas. Hemphill's. 183p.

French, B. M., and Short, N. M., 1968. Shock metamorphism of natural materials: Baltimore, Mono Book Corp., 644 p.

Gaither, T. A., Hagerty, J. J., and Bailen, M. 2015. The USGS Flynn Creek crater drill core collection: progress on a web-based portal and online database for the planetary science community (abstract #2089). 46th Lunar and Planetary Science Conference.

Hagerty, J. J., HcHone, J. F., and Gaither, T. A. 2013. The Flynn Creek crater drill core collection at the USGS in Flagstaff, Arizona (abstract #2122). 47th Lunar and Planetary Science Conference.

Horton Jr. J. W., Powars D. S., and Gohn G. S. 2005. Studies of the Chesapeake Bay impact structure-Introduction and discussion. In Studies of the Chesapeake Bay impact structure—The USGS-NASA Langley corehole, Hampton, Virginia, and related coreholes and geophysical surveys, edited by Horton Jr. J. W., Powars D. S., and Gohn G. S., U. S. Geological Survey Professional Paper #1688.

Horton Jr. W. J., Ormö J., Powars D. S., and Gohn G. S. 2006. Chesapeake Bay impact structure:

Morphology, crater fill, and relevance for impact processes on Mars. Meteoritics and Planetary Science 41: 1613–1624.

King, D. T., Jr. and J. Ormö, 2011. Wetumpka – a marine target impact structure examined in the field and by shallow core drilling, in Garry, W.B., and J.E. Bleacher, eds., *Analogues for planetary exploration*: Boulder, Colorado, Geological Society of America, Special Paper 483, p. 287-300.

King, D. T., Jr., J. Ormö, L. W. Petruny, and T. L. Neathery, 2006. Role of sea water in the formation of the Late Cretaceous Wetumpka impact structure, inner Gulf Coastal Plain of Alabama, USA: *Meteoritics and Planetary Science*, 41:1625-1631.

King, D. T., Jr., Adrian, D. R., Ormö, J., Petruny, L. W., Hagerty, J. J., Gaither, T. A., and Jaret, S. J. 2015. Flynn Creek impact structure, Tennessee: its crater-filling breccia in comparison to two other small Paleozoic impact structures and their breccia units (abstract #260475). *GSA Abstracts with Programs* 47.

King, D.T., Jr., Petruny, L.W., De Marchi, L., Chinchalkar, N.S., and Adams, M.C., 2018, sub Crater breccias, Flynn Creek impact structure, Tennessee: (abstract #2494). 49th Lunar and Planetary Science Conference. CD-ROM.

Lindström, M., Shuvalov, V., and Ivanov, B., 2005, Lockne crater as a result of marine-target oblique impact: *Planetary and Space Science*, 53:803-815.

Mazzullo, J.M., Meyer, A., and Kidd, R.B., 1988. New sediment classification scheme for the Ocean Drilling Program. In Mazzullo, J.M., and Graham, A.G. (Eds.), Handbook for shipboard sedimentologists. ODP Tech. Note, 8:45–67.

Ormö, J. and Lindström, M. 2000. When a cosmic impact strikes the seabed. *Geological Magazine* 137:67-80.

Ormö, J., Sturkell, E., Lindström, M. 2007. Sedimentological analysis of resurge deposits at the Lockne and Tvären craters: clues to flow dynamics. *Meteoritics and Planetary Science* 42:1929-1943.

Ormö, J., Sturkell, E., Horton, J.W., Jr., Powars, D.S., and Edwards, L.E. 2009. Comparison of clast frequency and size in the Exmore sediment-clast breccia, Eyreville and Langley cores, Chesapeake Bay impact structure: clues to the resurge process. Edited by Gohn, G. S., Koeberl, C., Miller, K. G., and Reimold, W.U. *The ICDP-USGS deep drilling project in the Chesapeake Bay impact structure: results from the Eyreville coreholes*. Boulder, Colorado. Geological Society of America Special Paper 458, pp. 617-632.

Osinski, G.R., Spray, J.G., and Lee, P. 2005. Impactites of the Haughton impact structure, Devon Island, Canada High Artic: *Meteoritics & Planetary Science*, v. 40, p. 1789-1812.

Osinski. G.R., Grieve, R.A.F., Chanou, A., and Sapers, H.M., 2016. The suevite conundrum, part 1: The Ries suevite and Sudbury Onaping Formation compared: *Meteoritics & Planetary Science*, v.51, p. 2316-2333.

Roddy, D. J. 1966. The Paleozoic crater at Flynn Creek, Tennessee [dissertation]. Pasadena, California. California Institute of Technology. 232p.

Roddy, D. J. 1968. The Flynn Creek crater, Tennessee. Edited by French, B. M., and Short, N. M. *Shock and Metamorphism of Natural Materials*. Baltimore, Maryland. Mono Book Corporation. pp. 291–322.

Roddy, D. J. 1979. Structural deformation at the Flynn Creek impact crater, Tennessee: a preliminary report on deep drilling. *Lunar and Planetary Science* 10:2519-2534.

Roddy D. J. 1980. Completion of a Deep Drilling Program at the Flynn Creek Impact Crater, Tennessee (abstract #1335). *11th Lunar and Planetary Science Conference*.

Roddy D. J. 1990. Structure Contour Map Drawn on the Base of the Chattanooga Shale Flynn Creek Crater, Gainesboro Quadrangle, Tennessee. Edited by Hill W. T., Tennessee Division of Geology, Scale 1:12,000.

Scheiber, J. and Over, J. D. 2005. Sedimentary fill of the Late Devonian Flynn Creek crater: a hard target marine impact. Edited by Over, D. J., Morrow, J. R., and Wignall, P. B. *Understanding Late Devonian and Permian-Triassic Biotic and Climatic Events: Towards and Integrated Approach*. New York. Elsevier. pp. 51-69.

Smith, R. W. and Whitlatch, G. I. 1940. The phosphate resources of Tennessee. *Tennessee Department of Conservation, Division of Geology, Bull*. 48, 1.

Sturkell, E., Ormö, J., and Lepinette, A. 2013. Early modification stage (pre-resurge) sediment mobilization in the Lockne concentric, marine-target crater, Sweden. *Meteoritics and Planetary Science* 48:321-338.

Terry, R. D. and Chilingar, C. V. 1955. Comparison charts for visual estimation of percentage composition. *Journal of Sedimentary Petrology*, vol. 25, n. 3, p. 229-234.

U. S. Geological Survey, 2017. Mineral Resources On-Line Spatial Data. http://mrdata.usgs.gov

Wilson Jr. C. W. 1962. Stratigraphy and geologicc history of Middle Ordovician rocks of central Tennessee. *Bulletin of the Geological Society of America* 73:481-504.

Wilson, C. W., Jr. and Roddy, D. J., 1990. Geologic map and mineral resources summary of the Gainesboro quadrangle, Tennessee: Tennessee Division of Geology, GM 325-SW, Scale 1:24,000.

Table 3. Melt particles on FC77-3

| Melt fragments FC 77-3 | | | | | | | | |
|---|---|---|---|---|---|---|---|---|
| thin section | covered/uncovered | depth (~m) | melt 1 % | | | melt 2 % | | |
| | | | | size (mm) | shape | | size (mm) | shape |
| 3-5-B | uncovered | 7.8 | 1 | 0.68 | sub angular to sub rounded | 2 | 0.35 | rounded and "needle shape" |
| 3-5-A | covered | 7.9 | 0.5 | 0.95 | sub angular to sub rounded | 1 | 0.32 | rounded to sub rounded |
| 3-3-A | covered | 8.8 | 0 | 0 | | 0.75 | 0.05 | sub angular to rounded |
| 3-3-B1 | covered | 9 | 0.25 | 0.45 | sub rounded | 1 | 0.16 | sub angular to rounded |
| 3-3-B | covered | 9.2 | 0 | 0 | | 0.75 | 0.24 | sub angular to rounded |
| 3-2-A | covered | 10 | 0.5 | 0.36 | sub rounded | 0.5 | 0.01 | sub angular to rounded |
| 4-5-A | uncovered | 10.7 | 0.25 | 1.52 | sub rounded | 0.5 | 0.41 | sub rounded to rounded |
| 4-4-A | covered | 11.5 | 0 | 0 | | 0.25 | 0.38 | rounded |
| 4-4-B | covered | 11.7 | 0.25 | 0.79 | sub angular | 1 | 0.26 | rounded + irregular mass with flow texture |
| 4-3-A | covered | 12.5 | 0 | 0 | | 0.25 | 0.3 | sub rounded |
| 4-1-A | covered | 13.7 | 0.5 | 1.23 | sub rounded | 0.3 | 0.1 | rounded |
| 5-3-A | covered | 15 | 0 | 0 | | 0.75 | 0.1 | sub angular to sub rounded |
| 5-1-A | covered | 16.2 | 0 | 0 | | 0.5 | 0.06 | sub angular to sub rounded |
| 6-5-A | covered | 16.8 | 0 | 0 | | 0.25 | 0.075 | rounded |
| 6-5-B | covered | 17.2 | 0 | 0 | | 0.15 | 0.91 | "needle" |
| 6-1-A | covered | 19.4 | 0.5 | 1.98 | sub angular | 0.75 | 0.2 | sub rounded to rounded |
| 7-4-A | covered | 20.5 | 0 | 0 | | 0.25 | 0.18 | rounded |
| 7-3-B | covered | 21 | | | | 0.5 | 0.2 | sub rounded and "needle shape" |
| 7-3-A | covered | 21.5 | 0 | 0 | | 0 | 0 | |
| 7-1-A | covered | 22.3 | 0 | 0 | | 0.5 | 0.17 | rounded |
| 8-5-A | covered | 22.7 | 0 | 0 | | 1 | 0.35 | rounded but some angular and long |
| 8-5-B | covered | 22.8 | 0 | 0 | | 0 | 0 | |
| 8-4-A | covered | 23 | 0.5 | 0.34 | sub angular to sub rounded | 0.5 | 0.69 | sub rounded |
| 8-3-A | covered | 23.5 | 0 | 0 | | 0 | 0 | |
| 8-2-A | covered | 24.5 | 0.75 | 0.4 | angular to rounded | 1.5 | 0.32 | sub angular to sub rounded |
| 9-5-A | uncovered | 25.5 | 0 | 0 | | 0 | 0 | |
| 9-4-A | covered | 26 | 0 | 0 | | 0 | 0 | |
| 9-2-A | covered | 27.3 | 0 | 0 | | 1.5 | 0.12 | sub angular to sub rounded |
| 9-1A | covered | 27.8 | 0 | 0 | | 0 | 0 | |
| 10-4-A | covered | 29 | 0 | 0 | | 0 | 0 | |
| 10-3-A | covered | 29.8 | 0 | 0 | | 0 | 0 | |
| 10-2-A | covered | 30 | 0 | 0 | | 0 | 0 | |
| 11-5-A | covered | 31.5 | 0 | 0 | | 1.25 | 0.89 | sub rounded + irregular mass with flow texture |
| 11-4-A | covered | 32.3 | 0 | 0 | | 0 | 0 | |
| 11-4-B | covered | 32.5 | 0 | 0 | | 1 | 0.48 | sub rounded to rounded (some angular) |
| 11-3-A | uncovered | 33 | 0 | 0 | | 12.5 | 0.58 | rounded + irregular mass with flow texture |
| 11-1-A | covered | 34.2 | 0.3 | 0.34 | sub angular to sub rounded | 1 | 0.26 | rounded (some angular) |
| 12-5-A | covered | 34.45 | 0.5 | 1.19 | sub rounded | 0.75 | 0.19 | rounded but some angular (clear color) |
| 12-5-B' | uncovered | 34.45 | 30 | 15 | irregular and dispersed | 0 | 0 | |
| 12-4-A | covered | 35 | 0 | 0 | | 0 | 0 | |

Table 4. Melt particles on FC67-3

| Melt fragments FC 67-3 | | | | | | | | |
|---|---|---|---|---|---|---|---|---|
| thin section | covered/uncovered | depth (~m) | melt 1 % | | | melt 2 % | | |
| | | | | size (mm) | shape | | size (mm) | shape |
| 67-5-5-A | covered | 15.8 | 0 | 0 | | 0 | 0 | |
| 67-5-4-A | uncovered | 16.0 | 0 | 0 | | 0 | 0 | |
| 67-5-3-A | covered | 16.5 | 0 | 0 | | 0 | 0 | |
| 67-5-2-A | covered | 17.0 | 0 | 0 | | 0 | 0 | |
| 67-5-1-A | uncovered | 18.0 | 0 | 0 | | 0 | 0 | |
| 67-6-5-A | covered | 18.3 | 0 | 0 | | 0 | 0 | |
| 67-6-4-A | uncovered | 19.0 | 0 | 0 | | 0.5 | 0.05 | sub angular to rounded |
| 67-6-3-A | covered | 19.5 | 0 | 0 | | 0.75 | 0.06 | sub angular to rounded |
| 67-6-2-A | covered | 19.7 | 0 | 0 | | 0.75 | 0.06 | sub angular to rounded |
| 67-6-1-A | uncovered | 19.8 | 0 | 0 | | 1.25 | 0.12 | sub angular to rounded |
| 67-7-5-A | uncovered | 20.0 | 0.5 | 0.55 | sub angular | 1 | 0.5 | most rounded but some angular clear occurences |
| 67-7-4-A | uncovered | 20.5 | 0.75 | 0.64 | sub rounded | 1 | 0.3 | most rounded but some angular clear occurences |
| 97-7-3-A | uncovered | 20.8 | 1 | 1.34 | sub rounded | 0.75 | 0.37 | most rounded but some angular clear occurences |
| 67-7-3-B | covered | 21.0 | 1 | 0.7 | sub ang to sub rounded | 1 | 0.55 | rounded to sub rounded |
| 67-7-2-A | uncovered | 22.0 | 1.25 | 2 | sub ang to sub rounded | 0.25 | 0.19 | rounded |
| 67-7-1-A | covered | 23.0 | 0.75 | 0.3 | sub ang to sub rounded | 0.5 | 0.35 | most rounded but some angular clear occurences |
| 67-8-5-A | covered | 23.5 | 0.75 | 1.03 | ang to rounded | 0 | 0 | |
| 67-8-3-A | covered | 25.0 | 0 | 0 | | 0.2 | 0.49 | sub rounded |
| 67-8-1-A | uncovered | 26.0 | 1 | 0.95 | ang to sub ang | 0.5 | 0.13 | most rounded but some angular clear occurences |
| 67-9-5-A | covered | 26.5 | 0.5 | 0.5 | angular | 0.3 | 0.15 | sub rounded to rounded |
| 67-9-4-A | uncovered | 27.0 | 0 | 0 | | 0 | 0 | |
| 67-9-1-A | covered | 28.5 | 0.2 | 0.26 | sub angular | 0 | 0 | |
| 67-10-5-A | uncovered | 29.0 | 0.5 | 0.39 | sub rounded | 0 | 0 | |
| 67-10-3-A | covered | 30.0 | 0 | 0 | | 0 | 0 | |
| 67-10-1-A | covered | 31.0 | 0 | 0 | | 0 | 0 | |
| 67-10-1-B | uncovered | 31.5 | 0 | 0 | | 0 | 0 | |
| 67-11-5-A | covered | 32.0 | 0 | 0 | | 0 | 0 | |
| 67-11-1-A | covered | 34.5 | 0 | 0 | | 0 | 0 | |
| 67-13-4-A | covered | 39.0 | 0.5 | 1.06 | sub ang to sun rounded | 0 | 0 | |

Table 5. Deposit content on FC77-3

| | | | | | FC 77- 3 | | | | | | | | | | |
|---|---|---|---|---|---|---|---|---|---|---|---|---|---|---|---|
| thin section | covered/uncovered | depth (~m) | obs | carbonate class (dunham) | % total matrix | cc filled fractures | stylolites | qtz % | chalcedony % | brachiopod % | bryozoan % | trilobite % | :hinoderm | coral % | |
| 3-5-A | covered | 7.9 | contact | wackestone | 70 | | | 6 | 1.5 | 0 | 0 | 0 | 1 | 0 | |
| 3-3-A | covered | 8.8 | | mudstone | 100 | | | 0.7 | 0 | 0 | 0 | 0 | 0 | 0 | |
| 3-3-B1 | covered | 9 | | wackestone | 60 | | | 0.5 | 0.5 | 0.7 | 0 | 0 | 1.25 | 0.5 | |
| 3-3-B | covered | 9.2 | | wackestone | 55 | | | 0.25 | 0.5 | 0.7 | 0 | 0 | 0.7 | 0 | |
| 3-2-A | covered | 10 | | wackestone | 40 | | | 0.5 | 0.5 | 1 | 0.5 | 0.5 | 1 | 0 | |
| 4-5-A | uncovered | 10.7 | | rudstone | 30 | | | 0.7 | 0.5 | 1.5 | 0 | 0.7 | 1 | 2 | |
| 4-4-A | covered | 11.5 | | rudstone | 20 | | | 0.25 | 0.7 | 1 | 0.7 | 0.5 | 1 | 0.7 | |
| 4-4-B | covered | 11.7 | | mudstone | 20 | | | 0.5 | 1 | 1 | 0 | 0.5 | 1 | 1 | |
| 4-3-A | covered | 12.5 | | rudstone | 25 | | | 0.7 | 0.5 | 1 | 0.5 | 0.7 | 0.5 | 1 | |
| 4-1-A | covered | 13.7 | | rudstone | 15 | | | 0.5 | 0.3 | 1 | 0.7 | 0.7 | 0 | 0.5 | |
| 5-3-A | covered | 15 | | rudstone | 30 | | | 1 | 0.25 | 1.5 | 0.5 | 1 | 0.7 | 1 | |
| 5-1-A | covered | 16.2 | | floatstone | 55 | | | 0.5 | 0 | 1 | 0.5 | 1 | 0 | 0 | |
| 6-5-A | covered | 16.8 | | floatstone | 30 | | | 0.75 | 0.5 | 1.5 | 0.7 | 1 | 0 | 0.5 | |
| 6-5-B | covered | 17.2 | | mudstone | 45 | | | 0.7 | 0 | 5 | 1.5 | 0.5 | 1 | 0 | |
| 6-1-A | covered | 19.4 | | floatstone | 65 | | | 1.5 | 0 | 1 | 0.5 | 1 | 0 | 0.5 | |
| 7-4-A | covered | 20.5 | | floatstone | 60 | | | 1 | 0.5 | 1.5 | 1 | 1 | 0.5 | 0.5 | |
| 7-3-B | covered | 21 | | floatstone | 70 | | | 1 | 0 | 1 | 0.5 | 0.5 | 1 | 1.5 | |
| 7-3-A | covered | 21.5 | | floatstone | 65 | | | 0.7 | 0 | 3 | 1 | 1.5 | 1 | 1 | |
| 7-1-A | covered | 22.3 | | rudstone | 60 | | | 0.7 | 0.5 | 1.5 | 0.5 | 0.5 | 1 | 0.5 | |
| 8-5-A | covered | 22.7 | | wackestone | 90 | | | 0.5 | 0 | 1 | 0.5 | 0.5 | 8 | 0.5 | |
| 8-5-B | covered | 22.8 | | mudstone | 100 | | | 0.25 | 0 | 0 | 0 | 0 | 0 | 0 | |
| 8-4-A | covered | 23 | | mudstone | 45 | | | 1 | 0.25 | 1 | 0 | 0.75 | 0.7 | 0 | |
| 8-3-A | covered | 23.5 | | wackestone | 85 | | | 0.25 | 0 | 1 | 0.5 | 1 | 0 | 1 | |
| 8-2-A | covered | 24.5 | | wackestone | 90 | | | 1.25 | 0.5 | 0.75 | 0 | 0.5 | 0.5 | 0 | |
| 9-5-A | uncovered | 25.5 | | wackestone | 95 | | | 0.25 | 0 | 3 | 0.5 | 1 | 1 | 0 | |
| 9-4-A | covered | 26 | | mudstone | 65 | | | 0.5 | 0 | 3 | 1 | 1 | 0.5 | 0 | |
| 9-2-A | covered | 27.3 | | floatstone | 80 | | | 0.75 | 0 | 1.5 | 1 | 1 | 0.5 | 0 | |
| 9-1A | covered | 27.8 | | floatstone | 70 | | | 0.25 | 0 | 3 | 1.5 | 1 | 0.5 | 0 | |
| 10-4-A | covered | 29 | | mudstone | 100 | | | 0 | 0 | 0.5 | 0 | 0.25 | 0 | 0.25 | |
| 10-3-A | covered | 29.8 | | floatstone | 80 | | | 0.25 | 0 | 0.75 | 1.5 | 1 | 0.5 | 1 | |
| 10-2-A | covered | 30 | | mudstone | 90 | | | 0.25 | 0.5 | 0.5 | 1 | 0 | 0.5 | 0 | |
| 11-5-A | covered | 31.5 | | mudstone | 97 | | | 1 | 0 | 1 | 0 | 0 | 0.75 | 0.5 | |
| 11-4-A | covered | 32.3 | | mudstone | 90 | | | 0.5 | 0.25 | 1 | 0.5 | 1 | 1.5 | 0.5 | |
| 11-4-B | covered | 32.5 | | rudstone | 70 | | | 0.5 | 0 | 1.5 | 1.5 | 3 | 0.5 | 1 | |
| 11-3-A | uncovered | 33 | | floatstone | 99 | | | 4 | 0 | 0.5 | 0 | 0.5 | 0 | 1.5 | |
| 11-1-A | covered | 34.2 | | wackestone | 80 | | | 2 | 0 | 0.5 | 0 | 0 | 0 | 0 | |
| 12-5-A | covered | 34.45 | | wackestone | 85 | | | 1 | 0 | 0.5 | 0 | 0 | 0 | 0.5 | |

Table 6. Deposit content on FC67-3

| FC 67-3 | | | | | | | | | | | | | | |
|---|---|---|---|---|---|---|---|---|---|---|---|---|---|---|
| thin section | covered/uncovered | depth (~m) | obs | carbonate class (dunham) | total matr cc filled fractures | stylolites | qtz % | chalcedony % | brachiopod % | bryozoan % | pellets % | trilobite % | echinoderm % | coral % |
| 67-5-5A | covered | 15.8 | contact | mudstone/shale | 100 | | 0 | 0 | 0 | 0 | 0 | 0 | 0 | 0 |
| 67-5-4-A | uncovered | 16.0 | | mudstone | 100 | | 0.25 | 0 | 0 | 0 | 0 | 0 | 0 | 0 |
| 67-5-3-A | covered | 16.5 | | mudstone/shale | 100 | | 0.5 | 0 | 0 | 0 | 0 | 0 | 0 | 0 |
| 67-5-2-A | covered | 17.0 | | mudstone | 100 | | 0.5 | 0 | 0 | 0 | 0 | 0 | 0 | 0 |
| 67-5-1-A | uncovered | 18.0 | | mudstone | 100 | | 1 | 0 | 0 | 0 | 0 | 0 | 0 | 0 |
| 67-6-5-A | covered | 18.3 | | mudstone | 100 | | 1 | 0 | 0 | 0 | 0 | 0 | 0 | 0 |
| 67-6-4-A | uncovered | 19.0 | | mudstone | 100 | | 3 | 0 | 0 | 0 | 0 | 0 | 0 | 0 |
| 67-6-3-A | covered | 19.5 | | mudstone | 100 | | 4 | 0 | 0 | 0 | 0 | 0 | 0 | 0 |
| 67-6-2-A | covered | 19.7 | | mudstone | 99 | | 4 | 0 | 0 | 0 | 0 | 0 | 0 | 0 |
| 67-6-1-A | uncovered | 19.8 | | mudstone | 99 | | 1.5 | 0 | 0 | 0 | 0 | 0 | 0 | 0 |
| 67-7-5-A | uncovered | 20.0 | | wackestone | 85 | | 1 | 0.25 | 0 | 0 | 0 | 0 | 0.75 | 0 |
| 67-7-4-A | uncovered | 20.5 | | wackestone | 85 | | 0.5 | 0 | 0 | 0 | 0 | 0 | 1.25 | 0 |
| 97-7-3-A | uncovered | 20.8 | | wackestone | 70 | | 1 | 0.25 | 0 | 0 | 0 | 0 | 1.25 | 0 |
| 67-7-3-B | covered | 21.0 | | shale | 70 | | 6 | 2 | 0 | 0 | 0 | 0.5 | 0.25 | 0 |
| 67-7-2-A | uncovered | 22.0 | | floatstone | 50 | | 2 | 1.25 | 2 | 0.5 | 0.5 | 0.3 | 0 | 0.3 |
| 67-7-1-A | covered | 23.0 | | rudstone | 45 | | 1 | 0.5 | 1 | 0.75 | 0.75 | 1 | 0.25 | 1 |
| 67-8-5-A | covered | 23.5 | | rudstone | 45 | | 1 | 1.5 | 1 | 0.5 | 0.5 | 1 | 0.5 | 1.5 |
| 67-8-3-A | covered | 25.0 | | rudstone | 50 | | 0.5 | 0.5 | 1.5 | 1 | 0.75 | 0.75 | 0.5 | 0.5 |
| 67-8-1-A | uncovered | 26.0 | | wackestone | 87 | | 1 | 0 | 0.5 | 0 | 0.5 | 0 | 0 | 0 |
| 67-9-5-A | covered | 26.5 | breecia-in-breccia | floatstone | 87 | | 0.5 | 0.75 | 0.5 | 0 | 0.3 | 0 | 0 | 0.5 |
| 67-9-4-A | uncovered | 27.0 | | floatstone | 60 | | 0.75 | 1 | 1.5 | 0.5 | 1 | 1 | 0.5 | 0.5 |
| 67-9-1-A | covered | 28.5 | | floatstone | 60 | | 0 | 0 | 0 | 0 | 0 | 0 | 0 | 0 |
| 67-10-5-A | uncovered | 29.0 | | floatstone | 50 | | 0 | 0.25 | 0 | 0 | 0 | 0 | 0 | 0 |
| 67-10-3-A | covered | 30.0 | | floatstone | 95 | | 0 | 0 | 0 | 0 | 0 | 0 | 0 | 0 |
| 67-10-1-A | covered | 31.0 | | floatstone | 65 | | 0 | 0 | 0 | 0 | 0 | 0 | 0 | 0 |
| 67-10-1-B | uncovered | 31.5 | | floatstone | 85 | | 0.25 | 0 | 0 | 0 | 0 | 0 | 0 | 0 |
| 67-11-5-A | covered | 32.0 | | mudstone | 99 | | 0 | 0 | 0 | 0 | 0 | 0 | 0 | 0 |
| 67-11-1-A | covered | 34.5 | | mudstone | 97 | | 0 | 0 | 0 | 0 | 0 | 0 | 0 | 0 |
| 67-13-4-A | covered | 39.0 | | floatstone | 80 | | 1 | 0.75 | 1 | 0.5 | 0.5 | 0.5 | 0.5 | 1 |